

## KINEMATIC AND DYNAMIC STUDY OF A MANIPULATOR 1T6R

*Liviu Marian Ungureanu*  
*IFToMM, Romania*  
*E-mail: ungureanu.liviu.marian@gmail.com*

*Elisabeta NICULAE*  
*IFToMM, Romania*  
*E-mail: banicaelisabeta29@yahoo.com*

*Florian Ion Tiberiu Petrescu*  
*IFToMM, Romania*  
*E-mail: fitpetrescu@gmail.com*

*Submission: 3/7/2021*  
*Accept: 12/1/2021*

### ABSTRACT

*The paper presents in detail a method of calculating the forces acting on a 1T6R robot manipulator. To determine the reactions (forces in kinematic torques), you must first determine the inertial forces in the mechanism to which one or more payloads of the robot can be added. The torsion of the inertial forces is calculated using the masses of the machine elements and the accelerations at the centers of mass of the elements of the mechanism, so that the positions, speeds, and accelerations acting on it, ie its complete kinematics, will be determined. Equations of the dynamics are also determined through an original method.*

**Keywords:** Robot; 1T6R robot; Forces; Kinematics; Dynamics

### 1. INTRODUCTION

Conveyor handling robots, or transport robots, have an important role in the industry because they repeat tiring movements, moving and transporting parts of different weights within a section, from one production stand to another, from one conveyor belt to one stand. processing, then to another conveyor belt or to another stand until the respective part of the respective subassembly will reach the general assembly section where it will be assembled in various subassemblies which will, in turn, be joined in the newly produced car.

Such a robot has the ability to recognize obstacles on its route inside the factory or section where it works and to integrate other environmental information into route planning. If necessary, change your trajectory so that you can always reach your destination as quickly as possible. Thus,

the robot contributes to the further improvement of safety at work and the efficiency of transport processes within the factory.

In a single trip, such a mobile transport robot can carry a load of up to 130 kg and choose the correct routes completely autonomously. Unlike traditional automatic transport systems, it does not require trajectory guidance in the form of induction loops, magnetic strips, or reflectors. To learn the route, the vehicle must be guided only once between stations, using a tablet or joystick. Thus, it registers itself to the environment and the changes in the surroundings and adapts its trajectory in case of need.

The robot navigates its environment with the help of sophisticated state-of-the-art technology: using sensors and laser scanners, it recognizes vehicles and immobile obstacles, as well as people who get in its way. The control system calculates the approach speed and detects the imminence of a collision. In this case, the robot stops itself or performs an avoidance action. Unlike other systems used, it immediately adapts its route based on environmental information, without having to stop during the process. If the fully autonomous robot detects that it will regularly encounter obstacles at a specific point in its trajectory, it changes its route permanently. If necessary, the electrically operated system can be moved to all destinations within the factory.

The robot can make about 120 trips a day and travels a total distance of 35 km on its route between the mechanical measurement center and the processing equipment for example.

Such a robotic system is called a cooperative. A handling robot also supplies dozens of machines and transports empty containers back to the warehouse (Antonescu; Petrescu, 1985; 1989; Antonescu et al., 1985a; 1985b; 1986; 1987; 1988; 1994; 1997; 2000a; 2000b; 2001; Atefi et al., 2008; Avaei et al., 2008; Aversa et al., 2017a; 2017b; 2017c; 2017d; 2017e; 2016a; 2016b; 2016c; 2016d; 2016e; 2016f; 2016g; 2016h; 2016i; 2016j; 2016k; 2016l; 2016m; 2016n; 2016o; Azaga; Othman, 2008; Cao et al., 2013; Dong et al., 2013; El-Tous, 2008; Comanescu, 2010; Franklin, 1930; He et al., 2013; Jolgaf et al., 2008; Kannappan et al., 2008; Lee, 2013; Lin et al., 2013; Liu et al., 2013; Meena AND Rittidech, 2008; Meena et al., 2008; Mirsayar et al., 2017; Ng et al., 2008; Padula; Perdereau; Pannirselvam, 2008; 2013; Perumaal; Jawahar, 2013; Petrescu, 2011; 2015a; 2015b; Petrescu; Petrescu, 1995a; 1995b; 1997a; 1997b; 1997c; 2000a; 2000b; 2002a; 2002b; 2003; 2005a; 2005b; 2005c; 2005d; 2005e; 2011a; 2011b; 2012a; 2012b; 2013a; 2013b; 2016a; 2016b; 2016c; Petrescu et al., 2009; 2016; 2017a; 2017b; 2017c; 2017d; 2017e; 2017f; 2017g; 2017h; 2017i; 2017j; 2017k; 2017l; 2017m; 2017n; 2017o; 2017p; 2017q; 2017r; 2017s; 2017t; 2017u; 2017v; 2017w; 2017x; 2017y; 2017z;



2017aa; 2017ab; 2017ac; 2017ad; 2017ae; 2018a; 2018b; 2018c; 2018d; 2018e; 2018f; 2018g; 2018h; 2018i; 2018j; 2018k; 2018l; 2018m; 2018n; Pourmahmoud, 2008; Rajasekaran et al., 2008; Shojaeeefard et al., 2008; Taher et al., 2008; Tavallaei; Tousi, 2008; Theansuwan; Triratanasirichai, 2008; Zahedi et al., 2008; Zulkifli et al., 2008).

## 2. METHODS AND MATERIALS

The present study will start with a description of the 1T6R robot proposed to be analyzed, in terms of the forces acting on it. The kinematics will be exemplified for the following dimensions of the 1T6R manipulator robot:

$l_1 = 0.1$  [m];  $l_3 = 0.8$  [m];  $l_2 = 1.1$  [m];  $a = 0.5$  [m];  $b = 0.6$  [m];  $l_4 = 0.7$  [m];  $x_O = 0$  [m];  $y_O = 0$  [m];  $y_E = 0$  [m];  $x_A = -0.5$  [m];  $y_A = -0.6$  [m];  $n = n_1 = 200$  [rot / min], for a complete rotation of the angle  $\varphi_1$  [deg] of the input element 1.

It is necessary to determine kinematically the transmission functions of the robot mechanism as well as the output angles:  $\varphi_2$  [deg];  $\varphi_3$  [deg];  $\varphi_4$  [deg]; together with the kinematic parameter of scalar coordinate type  $x_E$  [m].

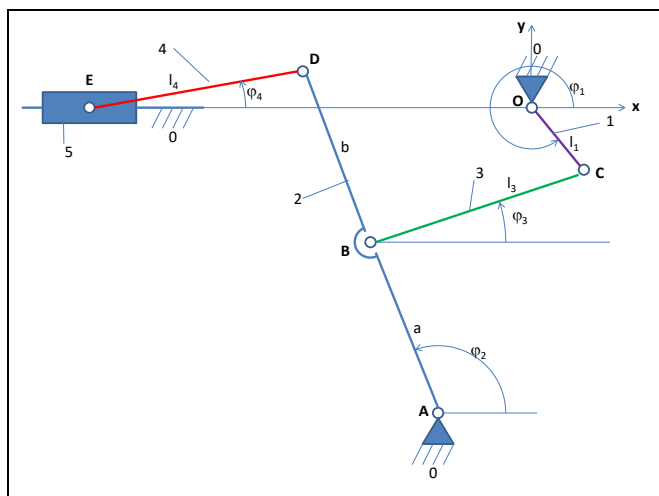


Figure 1: The mechanism 1T6R

Determination of positions and displacements:

A: Calculate crank 1 (1):

$$\begin{cases} x_C = x_O + l_1 \cdot \cos \varphi_1 \\ y_C = y_O + l_1 \cdot \sin \varphi_1 \end{cases} \quad (1)$$

B: Calculate the mechatronic module 3R (RRR):

For the 3R module, the calculation relations below (2) and figure 2 are used.

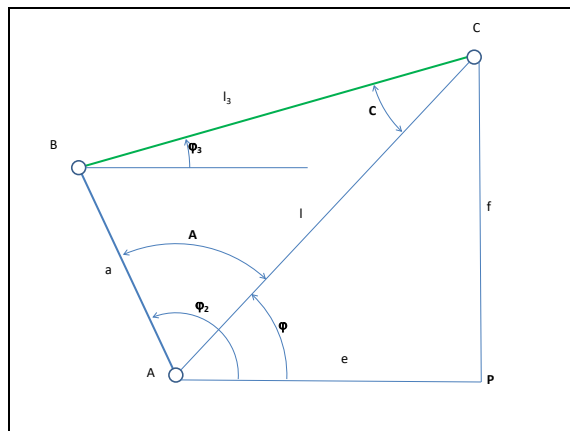


Figure 2: The mechanism of the dyad 2-3, of the robot 1T6R

$$\left\{ \begin{array}{l} e = x_C - x_A; f = y_C - y_A; l = \sqrt{e^2 + f^2} \\ \cos \varphi = \frac{e}{l}; \sin \varphi = \frac{f}{l}; \varphi = \arccos(\cos \varphi) \cdot \text{sign}(\sin \varphi) \\ \cos A = \frac{l^2 + a^2 - l_3^2}{2a \cdot l} \Rightarrow A = \arccos(\cos A) \\ \cos C = \frac{l^2 + l_3^2 - a^2}{2l \cdot l_3} \Rightarrow C = \arccos(\cos C) \\ \varphi_2 = \varphi + A \\ \varphi_3 = \varphi - C \\ x_D = x_A + l_2 \cdot \cos \varphi_2 \\ y_D = y_A + l_2 \cdot \sin \varphi_2 \end{array} \right. \quad (2)$$

C: Calculate the mechatronic RRT module

We can write:

$$\left\{ \begin{array}{l} x_D = x_E + l_4 \cdot \cos \varphi_4 \Rightarrow x_D - x_E = l_4 \cdot \cos \varphi_4 \Rightarrow (x_D - x_E)^2 + (y_D - y_E)^2 = l_4^2 \Rightarrow \\ y_D = y_E + l_4 \cdot \sin \varphi_4 \Rightarrow y_D - y_E = l_4 \cdot \sin \varphi_4 \\ \Rightarrow (x_D - x_E)^2 = l_4^2 - (y_D - y_E)^2 \Rightarrow x_E \end{array} \right. \quad (3)$$

The calculation equations (4) are obtained as follows:

$$\left\{ \begin{array}{l} x_E = x_D - \sqrt{l_4^2 - (y_D - y_E)^2} \\ \cos \varphi_4 = \frac{x_D - x_E}{l_4} \\ \sin \varphi_4 = \frac{y_D - y_E}{l_4} \\ \varphi_4 = \arccos(\cos \varphi_4) \cdot sign \\ (\sin \varphi_4) \end{array} \right. \quad (4)$$

Determination of speeds and accelerations:

The speeds and accelerations of the main elements and points in the mechanism are determined by the relationships below (5).

$$\left\{ \begin{array}{l} \omega_1 = 2\pi \cdot v_1 = \frac{\pi \cdot n_1}{30}; \quad \left\{ \begin{array}{l} \dot{x}_C = -l_1 \cdot \sin \varphi_1 \cdot \omega_1; \\ \dot{y}_C = l_1 \cdot \cos \varphi_1 \cdot \omega_1 \end{array} \right. ; \quad \left\{ \begin{array}{l} \ddot{x}_C = -l_1 \cdot \cos \varphi_1 \cdot \omega_1^2; \\ \ddot{y}_C = -l_1 \cdot \sin \varphi_1 \cdot \omega_1^2 \end{array} \right. ; \quad \left\{ \begin{array}{l} \dot{x}_A = 0; \\ \dot{y}_A = 0 \end{array} \right. ; \quad \left\{ \begin{array}{l} \ddot{x}_A = 0 \\ \ddot{y}_A = 0 \end{array} \right. \\ \left\{ \begin{array}{l} x_B = x_A + a \cdot \cos \varphi_2; \\ y_B = y_A + a \cdot \sin \varphi_2 \end{array} \right. ; \quad \left\{ \begin{array}{l} \dot{x}_B = -a \cdot \sin \varphi_2 \cdot \omega_2; \\ \dot{y}_B = a \cdot \cos \varphi_2 \cdot \omega_2 \end{array} \right. ; \quad \left\{ \begin{array}{l} \ddot{x}_B = -a \cdot \cos \varphi_2 \cdot \omega_2^2 - a \cdot \sin \varphi_2 \cdot \varepsilon_2 \\ \ddot{y}_B = -a \cdot \sin \varphi_2 \cdot \omega_2^2 + a \cdot \cos \varphi_2 \cdot \varepsilon_2 \end{array} \right. \\ \left\{ \begin{array}{l} x_D = x_E + l_4 \cdot \cos \varphi_4 \\ y_D = y_E + l_4 \cdot \sin \varphi_4 \end{array} \right. \quad \left\{ \begin{array}{l} \dot{x}_D = \dot{x}_E - l_4 \cdot \sin \varphi_4 \cdot \dot{\varphi}_4 \Rightarrow \dot{x}_E = \dot{x}_D + l_4 \cdot \sin \varphi_4 \cdot \dot{\varphi}_4 \\ \dot{y}_D = l_4 \cdot \cos \varphi_4 \cdot \dot{\varphi}_4 \Rightarrow \dot{\varphi}_4 = \frac{\dot{y}_D}{l_4 \cdot \cos \varphi_4} \end{array} \right. \\ \left\{ \begin{array}{l} \ddot{x}_D = \ddot{x}_E - l_4 \cdot \cos \varphi_4 \cdot \dot{\varphi}_4^2 - l_4 \cdot \sin \varphi_4 \cdot \ddot{\varphi}_4 \Rightarrow \ddot{x}_E = \ddot{x}_D + l_4 \cdot \cos \varphi_4 \cdot \dot{\varphi}_4^2 + l_4 \cdot \sin \varphi_4 \cdot \ddot{\varphi}_4 \\ \ddot{y}_D = -l_4 \cdot \sin \varphi_4 \cdot \dot{\varphi}_4^2 + l_4 \cdot \cos \varphi_4 \cdot \ddot{\varphi}_4 \Rightarrow \ddot{\varphi}_4 = \frac{\ddot{y}_D + l_4 \cdot \sin \varphi_4 \cdot \dot{\varphi}_4^2}{l_4 \cdot \cos \varphi_4} \end{array} \right. \\ \omega_2 = \frac{(\dot{x}_C - \dot{x}_A) \cdot \cos \varphi_3 + (\dot{y}_C - \dot{y}_A) \cdot \sin \varphi_3}{a \cdot \sin(\varphi_3 - \varphi_2)} = -\frac{l_1}{a} \cdot \frac{\sin(\varphi_1 - \varphi_3)}{\sin(\varphi_3 - \varphi_2)} \cdot \omega_1 \\ \omega_3 = \frac{(\dot{x}_C - \dot{x}_A) \cdot \cos \varphi_2 + (\dot{y}_C - \dot{y}_A) \cdot \sin \varphi_2}{l_3 \cdot \sin(\varphi_2 - \varphi_3)} = -\frac{l_1}{l_3} \cdot \frac{\sin(\varphi_1 - \varphi_2)}{\sin(\varphi_2 - \varphi_3)} \cdot \omega_1 \\ \omega_4 = \frac{\dot{y}_D}{l_4 \cdot \cos \varphi_4} \\ \varepsilon_2 = \frac{(\ddot{x}_C - \ddot{x}_A) \cdot \cos \varphi_3 + (\ddot{y}_C - \ddot{y}_A) \cdot \sin \varphi_3 + a \cdot \omega_2^2 \cdot \cos(\varphi_3 - \varphi_2) + l_3 \cdot \omega_3^2}{a \cdot \sin(\varphi_3 - \varphi_2)} \\ \varepsilon_3 = \frac{(\ddot{x}_C - \ddot{x}_A) \cdot \cos \varphi_2 + (\ddot{y}_C - \ddot{y}_A) \cdot \sin \varphi_2 + a \cdot \omega_2^2 + l_3 \cdot \omega_3^2 \cdot \cos(\varphi_2 - \varphi_3)}{l_3 \cdot \sin(\varphi_2 - \varphi_3)} \\ \varepsilon_4 = \frac{\ddot{y}_D + l_4 \cdot \sin \varphi_4 \cdot \dot{\varphi}_4^2}{l_4 \cdot \cos \varphi_4} \end{array} \right. \quad (5)$$

### Kinetostatics of a Planet Conveyor Manipulator

(Forces of a Conveyor Manipulator)



Determining the forces acting within a mechanism is an extremely important issue because based on these forces calculated before the respective mechanism is designed, the functional constructive parameters of the respective device can be anticipated. The greater the forces that will act in the kinematic torques of the mechanism, the more rigid a construction will be required for the elements of the respective mechanism, each element being designed to withstand both static and dynamic stresses in operation.

The motor or, as the case may be, the necessary drive motors are chosen, which can generate the necessary motor moments, these being superior to those during operation, also precalculated with the help of the previously determined mechanical forces. The forces in any device require all its components the demands being generally higher during operation, they generally increase with the square of the rotational speed of the main engine. The stresses depend very much on the inertial forces in the mechanism, which in turn increase with the speed of the mechanism (speed of the drive motor).

Each coupling imposes a certain type of movement and has an important influence on the dynamic mode of operation on the area and the entire kinematic chain. For this reason, the forces in the mechanism depend primarily on the type of mechanism, its torques, and elements, but also on the speed of the driving element.

The known external forces that act within any mechanism are those of inertia, together called the torsor of inertial forces (Figure 3). In the conveyor handling mechanism presented in this paper, the inertial forces are calculated using the relations belonging to system 6 (In the diagrams presented they are shown with a solid line (green), while the unknown forces to be determined, ie the reactions in the kinematic torques, are represented by the dashed line (red)).

$$\left\{ \begin{array}{l} F_{G_4}^{ix} = -m_4 \cdot \ddot{x}_{G_4} \\ F_{G_4}^{iy} = -m_4 \cdot \ddot{y}_{G_4} \\ M_4^i = -J_{G_4} \cdot \ddot{\phi}_4 \\ F_{G_5}^{ix} = -m_5 \cdot \ddot{x}_E \end{array} \right. \quad \left\{ \begin{array}{l} F_{G_2}^{ix} = -m_2 \cdot \ddot{x}_{G_2} \\ F_{G_2}^{iy} = -m_2 \cdot \ddot{y}_{G_2} \\ M_2^i = -J_{G_2} \cdot \ddot{\phi}_2 \end{array} \right. \quad \left\{ \begin{array}{l} F_{G_3}^{ix} = -m_3 \cdot \ddot{x}_{G_3} \\ F_{G_3}^{iy} = -m_3 \cdot \ddot{y}_{G_3} \\ M_3^i = -J_{G_3} \cdot \ddot{\phi}_3 \end{array} \right. \quad (6)$$

The force calculations are performed inversely than the kinematic ones, ie it starts with the last module of the mechanism (RRT) relational system 7, continues with the middle module (RRR) relational system 8, and ends with the leading element (system relations 9).

$$\left\{ \begin{array}{l} \sum M_D^{(4,5)} = 0 \Rightarrow -R_{05} \cdot (x_D - x_E) + F_{G_5}^{ix} \cdot (y_D - y_E) + F_{G_4}^{ix} \cdot (y_D - y_{G_4}) - F_{G_4}^{iy} \cdot (x_D - x_{G_4}) + M_4^i = 0 \\ \Rightarrow R_{05} = \frac{F_{G_5}^{ix} \cdot (y_D - y_E) + F_{G_4}^{ix} \cdot (y_D - y_{G_4}) - F_{G_4}^{iy} \cdot (x_D - x_{G_4}) + M_4^i}{x_D - x_E} \end{array} \right. \quad (7)$$

$$\left\{ \begin{array}{l} \sum F^{y(5)} = 0 \Rightarrow R_{05} + R_{45}^y = 0 \Rightarrow R_{45}^y = -R_{05} \Rightarrow R_E^y \equiv R_{54}^y = -R_{45}^y = R_{05} \\ \sum F^{x(5)} = 0 \Rightarrow F_{G_5}^{ix} + R_{45}^x = 0 \Rightarrow R_{45}^x = -F_{G_5}^{ix} \Rightarrow R_E^x \equiv R_{54}^x = -R_{45}^x = F_{G_5}^{ix} \end{array} \right.$$

$$\left\{ \begin{array}{l} \sum F^{y(4)} = 0 \Rightarrow R_{54}^y + F_{G_4}^{iy} + R_{24}^y = 0 \Rightarrow R_{24}^y = -R_{54}^y - F_{G_4}^{iy} = -R_{05} - F_{G_4}^{iy} \Rightarrow R_D^y \equiv R_{42}^y = -R_{24}^y = R_{05} + F_{G_4}^{iy} \\ \sum F^{x(4)} = 0 \Rightarrow R_{54}^x + F_{G_4}^{ix} + R_{24}^x = 0 \Rightarrow R_{24}^x = -R_{54}^x - F_{G_4}^{ix} = -F_{G_5}^{ix} - F_{G_4}^{ix} \Rightarrow R_D^x \equiv R_{42}^x = -R_{24}^x = F_{G_5}^{ix} + F_{G_4}^{ix} \end{array} \right.$$

$$\left\{ \begin{array}{l} \sum M_B^{(2)} = 0 \Rightarrow R_{02}^x \cdot (y_B - y_A) + R_{02}^y \cdot (x_A - x_B) - R_{42}^x \cdot (y_D - y_B) \\ - R_{42}^y \cdot (x_B - x_D) + F_{G_2}^{ix} \cdot (y_B - y_{G_2}) + F_{G_2}^{iy} \cdot (x_{G_2} - x_B) + M_2^i = 0 \end{array} \right.$$

$$\left\{ \begin{array}{l} \sum M_C^{(2,3)} = 0 \Rightarrow R_{02}^x \cdot (y_C - y_A) - R_{02}^y \cdot (x_C - x_A) - R_{42}^x \cdot (y_D - y_C) - R_{42}^y \cdot (x_C - x_D) + F_{G_2}^{ix} \cdot (y_C - y_{G_2}) \\ - F_{G_2}^{iy} \cdot (x_C - x_{G_2}) + M_2^i + F_{G_3}^{ix} \cdot (y_C - y_{G_3}) - F_{G_3}^{iy} \cdot (x_C - x_{G_3}) + M_3^i = 0 \end{array} \right.$$

$$\left\{ \begin{array}{l} \begin{cases} a_{11} \cdot R_{02}^x + a_{12} \cdot R_{02}^y = a_1 \\ a_{21} \cdot R_{02}^x + a_{22} \cdot R_{02}^y = a_2 \end{cases} \\ a_{11} = y_B - y_A \quad a_{12} = x_A - x_B \\ a_1 = R_{42}^x \cdot (y_D - y_B) + R_{42}^y \cdot (x_B - x_D) + F_{G_2}^{ix} \cdot (y_{G_2} - y_B) + F_{G_2}^{iy} \cdot (x_B - x_{G_2}) - M_2^i \\ a_{21} = y_C - y_A \quad a_{22} = x_A - x_C \\ a_2 = R_{42}^x \cdot (y_D - y_C) + R_{42}^y \cdot (x_C - x_D) + F_{G_2}^{ix} \cdot (y_{G_2} - y_C) + F_{G_2}^{iy} \cdot (x_C - x_{G_2}) - M_2^i \\ + F_{G_3}^{ix} \cdot (y_{G_3} - y_C) + F_{G_3}^{iy} \cdot (x_C - x_{G_3}) - M_3^i \end{array} \right.$$

$$\Delta = \begin{vmatrix} a_{11} & a_{12} \\ a_{21} & a_{22} \end{vmatrix} = a_{11} \cdot a_{22} - a_{12} \cdot a_{21} \quad \Delta_x = \begin{vmatrix} a_1 & a_{12} \\ a_2 & a_{22} \end{vmatrix} = a_1 \cdot a_{22} - a_2 \cdot a_{12} \quad \Delta_y = \begin{vmatrix} a_{11} & a_1 \\ a_{21} & a_2 \end{vmatrix} = a_2 \cdot a_{11} - a_1 \cdot a_{21}$$

$$R_A^x \equiv R_{02}^x = \frac{\Delta_x}{\Delta} \quad R_A^y \equiv R_{02}^y = \frac{\Delta_y}{\Delta}$$

$$\left\{ \begin{array}{l} \sum F^{x(2)} = 0 \Rightarrow R_{32}^x + R_{42}^x + R_{02}^x + F_{G_2}^{ix} = 0 \Rightarrow R_{32}^x = -R_{42}^x - R_{02}^x - F_{G_2}^{ix} \Rightarrow R_B^x \equiv R_{23}^x = -R_{32}^x \\ \sum F^{y(2)} = 0 \Rightarrow R_{32}^y + R_{42}^y + R_{02}^y + F_{G_2}^{iy} = 0 \Rightarrow R_{32}^y = -R_{42}^y - R_{02}^y - F_{G_2}^{iy} \Rightarrow R_B^y \equiv R_{23}^y = -R_{32}^y \\ \sum F^{x(3)} = 0 \Rightarrow R_{23}^x + F_{G_3}^{ix} + R_{13}^x = 0 \Rightarrow R_{13}^x = -R_{23}^x - F_{G_3}^{ix} \Rightarrow R_C^x \equiv R_{31}^x = -R_{13}^x \\ \sum F^{y(3)} = 0 \Rightarrow R_{23}^y + F_{G_3}^{iy} + R_{13}^y = 0 \Rightarrow R_{13}^y = -R_{23}^y - F_{G_3}^{iy} \Rightarrow R_C^y \equiv R_{31}^y = -R_{13}^y \end{array} \right.$$

$$\left\{ \begin{array}{l} \sum M_m^{(1)} = 0 \Rightarrow M_m + R_{31}^x \cdot (y_O - y_C) + R_{31}^y \cdot (x_C - x_O) = 0 \Rightarrow M_m = R_{31}^x \cdot (y_C - y_O) + R_{31}^y \cdot (x_O - x_C) \\ \sum F^{x(1)} = 0 \Rightarrow R_{01}^x + R_{31}^x = 0 \Rightarrow R_O^x \equiv R_{01}^x = -R_{31}^x \\ \sum F^{y(1)} = 0 \Rightarrow R_{01}^y + R_{31}^y = 0 \Rightarrow R_O^y \equiv R_{01}^y = -R_{31}^y \end{array} \right. \quad (9)$$

In relational system 10, the kinematic equations of the centers of gravity for elements 2, 3, and 4 are written. The center of gravity of element 1 coincides with point O because element 1 is totally statically balanced and the center of gravity of element 5 coincides with the joint E fact for which the moment M05 is zero.



$$\begin{aligned}
 & \left\{ \begin{array}{l} s_4 = \frac{2}{3} \cdot l_4 \quad s_2 = \frac{1}{3} \cdot (a+b) \quad s_3 = \frac{2}{3} \cdot l_3 \end{array} \right. \\
 & \left\{ \begin{array}{l} x_{G_3} = x_B + s_3 \cdot \cos \varphi_3 \quad \dot{x}_{G_3} = \dot{x}_B - s_3 \cdot \sin \varphi_3 \cdot \dot{\varphi}_3 \quad \ddot{x}_{G_3} = \ddot{x}_B - s_3 \cdot \cos \varphi_3 \cdot \dot{\varphi}_3^2 - s_3 \cdot \sin \varphi_3 \cdot \ddot{\varphi}_3 \\ y_{G_3} = y_B + s_3 \cdot \sin \varphi_3 \quad \dot{y}_{G_3} = \dot{y}_B + s_3 \cdot \cos \varphi_3 \cdot \dot{\varphi}_3 \quad \ddot{y}_{G_3} = \ddot{y}_B - s_3 \cdot \sin \varphi_3 \cdot \dot{\varphi}_3^2 + s_3 \cdot \cos \varphi_3 \cdot \ddot{\varphi}_3 \end{array} \right. \\
 & \left\{ \begin{array}{l} x_{G_2} = x_A + s_2 \cdot \cos \varphi_2 \quad \dot{x}_{G_2} = -s_2 \cdot \sin \varphi_2 \cdot \dot{\varphi}_2 \quad \ddot{x}_{G_2} = -s_2 \cdot \cos \varphi_2 \cdot \dot{\varphi}_2^2 - s_2 \cdot \sin \varphi_2 \cdot \ddot{\varphi}_2 \\ y_{G_2} = y_A + s_2 \cdot \sin \varphi_2 \quad \dot{y}_{G_2} = s_2 \cdot \cos \varphi_2 \cdot \dot{\varphi}_2 \quad \ddot{y}_{G_2} = -s_2 \cdot \sin \varphi_2 \cdot \dot{\varphi}_2^2 + s_2 \cdot \cos \varphi_2 \cdot \ddot{\varphi}_2 \end{array} \right. \\
 & \left\{ \begin{array}{l} x_{G_4} = x_E + s_4 \cdot \cos \varphi_4 \quad \dot{x}_{G_4} = \dot{x}_E - s_4 \cdot \sin \varphi_4 \cdot \dot{\varphi}_4 \quad \ddot{x}_{G_4} = \ddot{x}_E - s_4 \cdot \cos \varphi_4 \cdot \dot{\varphi}_4^2 - s_4 \cdot \sin \varphi_4 \cdot \ddot{\varphi}_4 \\ y_{G_4} = y_E + s_4 \cdot \sin \varphi_4 \quad \dot{y}_{G_4} = s_4 \cdot \cos \varphi_4 \cdot \dot{\varphi}_4 \quad \ddot{y}_{G_4} = -s_4 \cdot \sin \varphi_4 \cdot \dot{\varphi}_4^2 + s_4 \cdot \cos \varphi_4 \cdot \ddot{\varphi}_4 \end{array} \right. \\
 & \left\{ \begin{array}{l} x_D = x_A + (a+b) \cdot \cos \varphi_2 \quad \dot{x}_D = \dot{x}_A - (a+b) \cdot \sin \varphi_2 \cdot \omega_2 \quad \ddot{x}_D = \ddot{x}_A - (a+b) \cdot \cos \varphi_2 \cdot \omega_2^2 - (a+b) \cdot \sin \varphi_2 \cdot \varepsilon_2 \\ y_D = y_A + (a+b) \cdot \sin \varphi_2 \quad \dot{y}_D = \dot{y}_A + (a+b) \cdot \cos \varphi_2 \cdot \omega_2 \quad \ddot{y}_D = \ddot{y}_A - (a+b) \cdot \sin \varphi_2 \cdot \omega_2^2 + (a+b) \cdot \cos \varphi_2 \cdot \varepsilon_2 \end{array} \right. \\
 & \left\{ \begin{array}{l} x_D = x_E + l_4 \cdot \cos \varphi_4 \quad \dot{x}_D = \dot{x}_E - l_4 \cdot \sin \varphi_4 \cdot \dot{\varphi}_4 \Rightarrow \dot{x}_E = \dot{x}_D + l_4 \cdot \sin \varphi_4 \cdot \dot{\varphi}_4 \\ y_D = y_E + l_4 \cdot \sin \varphi_4 \quad \dot{y}_D = l_4 \cdot \cos \varphi_4 \cdot \dot{\varphi}_4 \Rightarrow \dot{\varphi}_4 = \frac{\dot{y}_D}{l_4 \cdot \cos \varphi_4} \end{array} \right. \\
 & \left\{ \begin{array}{l} \ddot{x}_D = \ddot{x}_E - l_4 \cdot \cos \varphi_4 \cdot \dot{\varphi}_4^2 - l_4 \cdot \sin \varphi_4 \cdot \ddot{\varphi}_4 \Rightarrow \ddot{x}_E = \ddot{x}_D + l_4 \cdot \cos \varphi_4 \cdot \dot{\varphi}_4^2 + l_4 \cdot \sin \varphi_4 \cdot \ddot{\varphi}_4 \\ \ddot{y}_D = -l_4 \cdot \sin \varphi_4 \cdot \dot{\varphi}_4^2 + l_4 \cdot \cos \varphi_4 \cdot \ddot{\varphi}_4 \Rightarrow \ddot{\varphi}_4 = \frac{\ddot{y}_D + l_4 \cdot \sin \varphi_4 \cdot \dot{\varphi}_4^2}{l_4 \cdot \cos \varphi_4} \end{array} \right. \\
 & \left\{ \begin{array}{l} m_2 = 0.3 \cdot (a+b) \quad m_3 = 0.3 \cdot l_3 \quad m_4 = 0.3 \cdot l_4 [kg] \quad m_5 = 0.5 [kg] \\ J_{G_2} = \frac{m_2 \cdot (a+b)^2}{12} \quad J_{G_3} = \frac{m_3 \cdot l_3^2}{12} \quad J_{G_4} = \frac{m_4 \cdot l_4^2}{12} [kg \cdot m^2] \end{array} \right. \tag{10}
 \end{aligned}$$

The relations with which the masses are determined (generally depending on the lengths of the respective elements) and the inertial masses of elements 2, 3, and 4 are also described. If m represents the mass of an element at its linear displacement and is measured in kg, J represents the rotational mass of the respective element determined around the axis of rotation, usually in the center of gravity of the respective element, and is measured in [kg.m<sup>2</sup>].

The rotational mass of an element (body or system of moving bodies) is extremely important, always completing the equations of motion of that body, having a major influence on its dynamics, and its final energy. The rotational mass of a body is generally less known than that of translation and for this reason, it is generally neglected in calculations. There are large errors in the equations of motion of that body, in its dynamics, or in determining the total kinetic energy of that body in translational motion plus rotation (the equations are also valid in the case of a material point, ie when determining the dynamics of elementary particles).



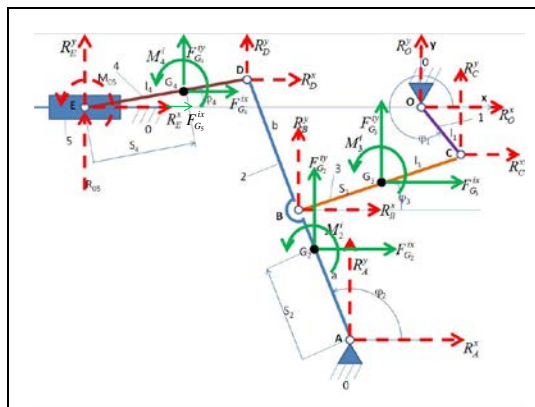


Figure 3: Forces acting on a simple conveyor manipulator

## 2.1. Determination of the mechanical (or mass: inertia: $J^*$ ) moment of the entire crank reduced mechanism 1

The moment of mass inertia of the whole mechanism (Figure 4) is determined exactly with the first relation of the relational system 11 below, but after all the necessary parameters have been calculated beforehand, on modules, with the help of the following relations from the composition of the system 11. Units of measurement are given in square brackets.

The mechanical or mass moment of inertia of the whole mechanism reduced to crank 1, does not depend on the input speed, it being only a positional function after the input variable FI1, and each student will calculate this parameter (measured in  $\text{kg} \cdot \text{m}^2$ ) for a single position, corresponding to its entrance angle,  $\varphi_1$ .

$$\begin{aligned}
 & \left\{ s_4 = \frac{2}{3} \cdot l_4; \quad s_2 = \frac{1}{3} \cdot (a + b); \quad s_3 = \frac{2}{3} \cdot l_3 [\text{m}] \right. \\
 & \left\{ m_1 [\text{kg}] = 2 \cdot 0,3 \cdot l_1; \quad J_{G_1} [\text{kg} \cdot \text{m}^2] = \frac{1}{2} \cdot m_1 \cdot l_1^2 \right. \\
 & \left\{ m_2 = 0,3 \cdot (a + b); \quad m_3 = 0,3 \cdot l_3; \quad m_4 = 0,3 \cdot l_4; \quad m_5 = 0,5 [\text{kg}] \right. \\
 & \left. J_{G_2} = \frac{m_2 \cdot (a + b)^2}{12}; \quad J_{G_3} = \frac{m_3 \cdot l_3^2}{12}; \quad J_{G_4} = \frac{m_4 \cdot l_4^2}{12} [\text{kg} \cdot \text{m}^2] \right. \\
 & J^* [\text{kg} \cdot \text{m}^2] = J_{G_1} + J_{G_3} \cdot \left( \frac{\omega_3}{\omega_1} \right)^2 + m_3 \cdot \left( \frac{v_{G_3}}{\omega_1} \right)^2 + J_{G_2} \cdot \left( \frac{\omega_2}{\omega_1} \right)^2 + m_2 \cdot \left( \frac{v_{G_2}}{\omega_1} \right)^2 + J_{G_4} \cdot \left( \frac{\omega_4}{\omega_1} \right)^2 + m_4 \cdot \left( \frac{v_{G_4}}{\omega_1} \right)^2 + m_5 \cdot \left( \frac{v_E}{\omega_1} \right)^2 \\
 & \frac{\omega_2}{\omega_1} = \frac{l_1}{a} \cdot \frac{\sin(\varphi_3 - \varphi_1)}{\sin(\varphi_3 - \varphi_2)} \\
 & \frac{\omega_3}{\omega_1} = \frac{l_1}{l_3} \cdot \frac{\sin(\varphi_2 - \varphi_1)}{\sin(\varphi_2 - \varphi_3)} \\
 & \frac{\omega_4}{\omega_1} = \frac{(a + b) \cdot l_1}{a \cdot l_4} \cdot \frac{\cos \varphi_2 \cdot \sin(\varphi_3 - \varphi_1)}{\cos \varphi_4 \cdot \sin(\varphi_3 - \varphi_2)} \\
 & \frac{v_{G_1}}{\omega_1} [\text{m}] = \frac{s_2 \cdot l_1}{a} \cdot \frac{\sin(\varphi_3 - \varphi_1)}{\sin(\varphi_3 - \varphi_2)} \\
 & \left( \frac{v_{G_1}}{\omega_1} \right)^2 [\text{m}^2] = \frac{l_1^2}{\sin^2(\varphi_3 - \varphi_2)} \cdot \left[ \sin^2(\varphi_3 - \varphi_1) + \frac{s_3^2}{l_3^2} \cdot \sin^2(\varphi_2 - \varphi_1) - \frac{2s_3}{l_3} \cdot \sin(\varphi_3 - \varphi_1) \cdot \sin(\varphi_2 - \varphi_1) \cdot \cos(\varphi_3 - \varphi_2) \right] \\
 & \frac{v_E}{\omega_1} [\text{m}] = \frac{l_1 \cdot (a + b)}{a} \cdot \frac{\sin(\varphi_3 - \varphi_1)}{\sin(\varphi_3 - \varphi_2)} \cdot (tg \varphi_4 \cdot \cos \varphi_2 - \sin \varphi_2) \\
 & \left( \frac{v_{G_4}}{\omega_1} \right)^2 [\text{m}^2] = \left( \frac{v_E}{\omega_1} \right)^2 + s_4^2 \cdot \left( \frac{\omega_4}{\omega_1} \right)^2 - 2 \cdot s_4 \cdot \sin \varphi_4 \cdot \frac{v_E}{\omega_1} \cdot \frac{\omega_4}{\omega_1}
 \end{aligned} \tag{11}$$

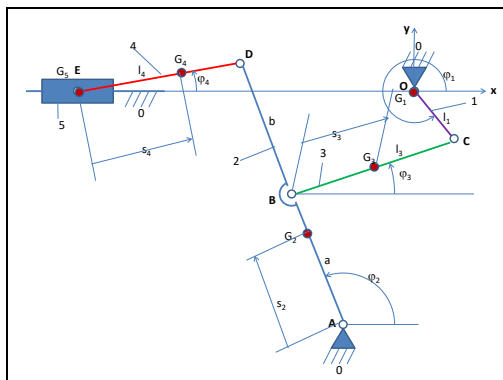


Figure 4: Determination of the centers of mass of the mechanism

The moment of mass inertia of the whole mechanism can be derived depending on the position angle FI1 of the crank, obtaining the calculation relations belonging to the relational system 12. Each student will calculate this parameter (measured in kg.m<sup>2</sup>) for a single position, corresponding to his entry angle, φ<sub>1</sub>.

$$\left\{ \begin{array}{l} J^* = \frac{2}{\omega_1^3} \cdot [J_{G_3} \cdot \varepsilon_3 \cdot \omega_3 + m_3 \cdot (\dot{x}_{G_3} \cdot \ddot{x}_{G_3} + \dot{y}_{G_3} \cdot \ddot{y}_{G_3}) + J_{G_2} \cdot \varepsilon_2 \cdot \omega_2 + m_2 \cdot (\dot{x}_{G_2} \cdot \ddot{x}_{G_2} + \dot{y}_{G_2} \cdot \ddot{y}_{G_2}) + \\ + J_{G_4} \cdot \varepsilon_4 \cdot \omega_4 + m_4 \cdot (\dot{x}_{G_4} \cdot \ddot{x}_{G_4} + \dot{y}_{G_4} \cdot \ddot{y}_{G_4}) + m_5 \cdot v_E \cdot a_E] \end{array} \right. \quad (12)$$

## 2.2. Dynamics of the mechanism

The moment of mass inertia of the whole mechanism in its average value is determined using the maximum and minimum functions, to find the maximum and minimum values, respectively, after which their arithmetic mean is made to determine the average value of the moment of mass inertia of the whole mechanism 1, J<sub>m</sub>\*.

In order not to complicate the calculations, this value is already considered known, it being: J<sub>m</sub>\* = 0,0297[kg · m<sup>2</sup>].

In dynamic calculations, we want to find out the real movement of the mechanism, when the angular velocity ω<sub>1</sub> of crank 1 is no longer constant but varies with both the speed and the position of the crank. This also causes a non-zero ε<sub>1</sub> value to appear.

Using some original dynamic equations, which also verifies the Lagrange ones (relational system III), they will be further determined with the help of system 13, the variable angular velocity ω<sub>1</sub> of the crank in the indicated position FI1, and the angular acceleration ε<sub>1</sub> for the same angle FI1 imposed on the crank 1.

$$\begin{cases} \omega_1^*[s^{-1}] = \sqrt{J_m^*} \cdot \omega_{n_1} \cdot \frac{1}{\sqrt{J^*}} \\ \varepsilon_1^*[s^{-2}] = -\frac{J_m^* \cdot \omega_{n_1}^2}{2} \cdot \frac{J^{*2}}{J^{*2}} \end{cases} \quad (13)$$

### 2.3. Dynamic Kinematics (partial)

$$\text{One has used: } s_4 = \frac{2}{3} \cdot l_4 \quad s_2 = \frac{1}{3} \cdot (a + b) \quad s_3 = \frac{2}{3} \cdot l_3$$

The dynamic velocities and the dynamic accelerations (in partial dynamics, without the influence of dynamic coefficients) of the main elements and points in the mechanism are determined by the relations below (14).

$$\begin{aligned} & \left\{ \begin{array}{l} \omega_1 = \omega_1^*; \quad \dot{x}_C = -l_1 \cdot \sin \varphi_1 \cdot \omega_1^*; \quad \ddot{x}_C = -l_1 \cdot \cos \varphi_1 \cdot \omega_1^{*2} - l_1 \cdot \sin \varphi_1 \cdot \varepsilon_1^*; \\ \dot{y}_C = l_1 \cdot \cos \varphi_1 \cdot \omega_1^*; \quad \ddot{y}_C = -l_1 \cdot \sin \varphi_1 \cdot \omega_1^{*2} + l_1 \cdot \cos \varphi_1 \cdot \varepsilon_1^*; \end{array} \right. \quad \left\{ \begin{array}{l} \dot{x}_A = 0; \quad \ddot{x}_A = 0 \\ \dot{y}_A = 0; \quad \ddot{y}_A = 0 \end{array} \right. \\ & \left\{ \begin{array}{l} \omega_{2D} = \frac{(\dot{x}_C - \dot{x}_A) \cdot \cos \varphi_3 + (\dot{y}_C - \dot{y}_A) \cdot \sin \varphi_3}{a \cdot \sin(\varphi_3 - \varphi_2)} = \frac{l_1}{a} \cdot \frac{\sin(\varphi_3 - \varphi_1)}{\sin(\varphi_3 - \varphi_2)} \cdot \omega_1^* \\ \omega_{3D} = \frac{(\dot{x}_C - \dot{x}_A) \cdot \cos \varphi_2 + (\dot{y}_C - \dot{y}_A) \cdot \sin \varphi_2}{l_3 \cdot \sin(\varphi_2 - \varphi_3)} = \frac{l_1}{l_3} \cdot \frac{\sin(\varphi_2 - \varphi_1)}{\sin(\varphi_2 - \varphi_3)} \cdot \omega_1^* \\ \varepsilon_{2D} = \frac{(\ddot{x}_C - \ddot{x}_A) \cdot \cos \varphi_3 + (\ddot{y}_C - \ddot{y}_A) \cdot \sin \varphi_3 + a \cdot \omega_{2D}^2 \cdot \cos(\varphi_3 - \varphi_2) + l_3 \cdot \omega_{3D}^2}{a \cdot \sin(\varphi_3 - \varphi_2)} \end{array} \right. \\ & \left\{ \begin{array}{l} x_B = x_A + a \cdot \cos \varphi_2; \quad \dot{x}_B = -a \cdot \sin \varphi_2 \cdot \omega_{2D}; \quad \ddot{x}_B = -a \cdot \cos \varphi_2 \cdot \omega_{2D}^2 - a \cdot \sin \varphi_2 \cdot \varepsilon_{2D} \\ y_B = y_A + a \cdot \sin \varphi_2; \quad \dot{y}_B = a \cdot \cos \varphi_2 \cdot \omega_{2D}; \quad \ddot{y}_B = -a \cdot \sin \varphi_2 \cdot \omega_{2D}^2 + a \cdot \cos \varphi_2 \cdot \varepsilon_{2D} \end{array} \right. \\ & \left\{ \begin{array}{l} x_D = x_A + (a+b) \cdot \cos \varphi_2 \quad \dot{x}_D = \dot{x}_A - (a+b) \cdot \sin \varphi_2 \cdot \omega_{2D} \\ y_D = y_A + (a+b) \cdot \sin \varphi_2 \quad \dot{y}_D = \dot{y}_A + (a+b) \cdot \cos \varphi_2 \cdot \omega_{2D} \end{array} \right. \\ & \left\{ \begin{array}{l} \ddot{x}_D = \ddot{x}_A - (a+b) \cdot \cos \varphi_2 \cdot \omega_{2D}^2 - (a+b) \cdot \sin \varphi_2 \cdot \varepsilon_{2D} \\ \ddot{y}_D = \ddot{y}_A - (a+b) \cdot \sin \varphi_2 \cdot \omega_{2D}^2 + (a+b) \cdot \cos \varphi_2 \cdot \varepsilon_{2D} \end{array} \right. \\ & \left\{ \begin{array}{l} \dot{\varphi}_{4D} \equiv \omega_{4D} = \frac{\dot{y}_D}{l_4 \cdot \cos \varphi_4} \\ \dot{x}_D = \dot{x}_E - l_4 \cdot \sin \varphi_4 \cdot \dot{\varphi}_4 \Rightarrow \dot{x}_{ED} = \dot{x}_D + l_4 \cdot \sin \varphi_4 \cdot \dot{\varphi}_{4D} \end{array} \right. \\ & \left\{ \begin{array}{l} \ddot{y}_D = -l_4 \cdot \sin \varphi_4 \cdot \dot{\varphi}_{4D}^2 + l_4 \cdot \cos \varphi_4 \cdot \ddot{\varphi}_{4D} \Rightarrow \ddot{\varphi}_{4D} \equiv \varepsilon_{4D} = \frac{\ddot{y}_D + l_4 \cdot \sin \varphi_4 \cdot \dot{\varphi}_{4D}^2}{l_4 \cdot \cos \varphi_4} \\ \ddot{x}_D = \ddot{x}_E - l_4 \cdot \cos \varphi_4 \cdot \dot{\varphi}_{4D}^2 - l_4 \cdot \sin \varphi_4 \cdot \ddot{\varphi}_{4D} \Rightarrow \ddot{x}_{ED} = \ddot{x}_D + l_4 \cdot \cos \varphi_4 \cdot \dot{\varphi}_{4D}^2 + l_4 \cdot \sin \varphi_4 \cdot \ddot{\varphi}_{4D} \end{array} \right. \\ & \varepsilon_{3D} = \frac{(\ddot{x}_C - \ddot{x}_A) \cdot \cos \varphi_2 + (\ddot{y}_C - \ddot{y}_A) \cdot \sin \varphi_2 + a \cdot \omega_{2D}^2 + l_3 \cdot \omega_{3D}^2 \cdot \cos(\varphi_2 - \varphi_3)}{l_3 \cdot \sin(\varphi_2 - \varphi_3)} \\ & \left\{ \begin{array}{l} \dot{x}_{G_3} = \dot{x}_B - s_3 \cdot \sin \varphi_3 \cdot \omega_{3D} \quad \ddot{x}_{G_3} = \ddot{x}_B - s_3 \cdot \cos \varphi_3 \cdot \omega_{3D}^2 - s_3 \cdot \sin \varphi_3 \cdot \varepsilon_{3D} \\ \dot{y}_{G_3} = \dot{y}_B + s_3 \cdot \cos \varphi_3 \cdot \omega_{3D} \quad \ddot{y}_{G_3} = \ddot{y}_B - s_3 \cdot \sin \varphi_3 \cdot \omega_{3D}^2 + s_3 \cdot \cos \varphi_3 \cdot \varepsilon_{3D} \end{array} \right. \\ & \left\{ \begin{array}{l} \dot{x}_{G_2} = -s_2 \cdot \sin \varphi_2 \cdot \omega_{2D} \quad \ddot{x}_{G_2} = -s_2 \cdot \cos \varphi_2 \cdot \omega_{2D}^2 - s_2 \cdot \sin \varphi_2 \cdot \varepsilon_{2D} \\ \dot{y}_{G_2} = s_2 \cdot \cos \varphi_2 \cdot \omega_{2D} \quad \ddot{y}_{G_2} = -s_2 \cdot \sin \varphi_2 \cdot \omega_{2D}^2 + s_2 \cdot \cos \varphi_2 \cdot \varepsilon_{2D} \end{array} \right. \\ & \left\{ \begin{array}{l} \dot{x}_{G_4} = \dot{x}_E - s_4 \cdot \sin \varphi_4 \cdot \omega_{4D} \quad \ddot{x}_{G_4} = \ddot{x}_E - s_4 \cdot \cos \varphi_4 \cdot \omega_{4D}^2 - s_4 \cdot \sin \varphi_4 \cdot \varepsilon_{4D} \\ \dot{y}_{G_4} = s_4 \cdot \cos \varphi_4 \cdot \omega_{4D} \quad \ddot{y}_{G_4} = -s_4 \cdot \sin \varphi_4 \cdot \omega_{4D}^2 + s_4 \cdot \cos \varphi_4 \cdot \varepsilon_{4D} \end{array} \right. \end{aligned} \quad (14)$$



### 3. RESULTS AND DISCUSSION

The diagram in figure 5 shows the angular displacements of the elements 2, 3, and 4, FI2 [deg], FI3 [deg], FI4 [deg], and the displacement of the point E in translational motion (given by the coordinate along the axis x of the point E ), xE [dm], depending on the rotation angle FI1.

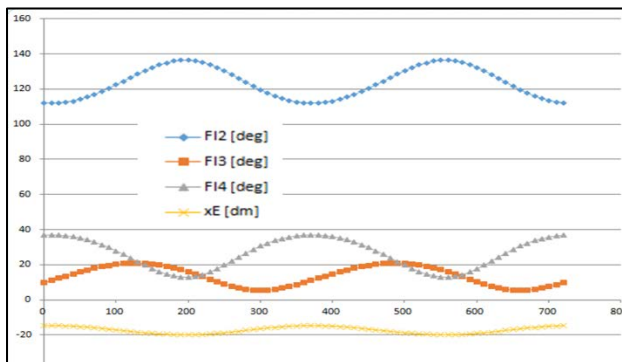


Figure 5: Variation of displacements depending on the rotation angle FI1

The variation of the speeds is shown in the diagrams in figure 6 and that of the respective accelerations in the diagrams in figure 7.

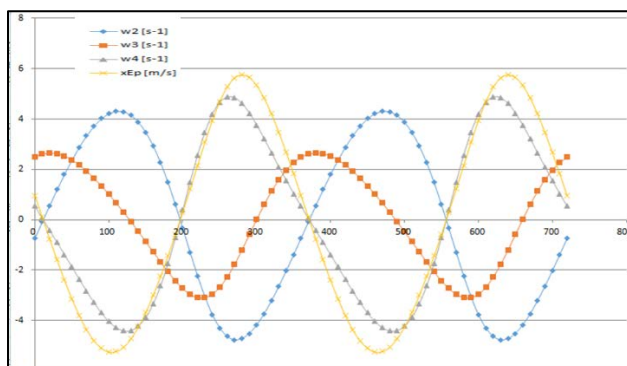


Figure 6: Variation of velocities depending on the rotation angle FI1

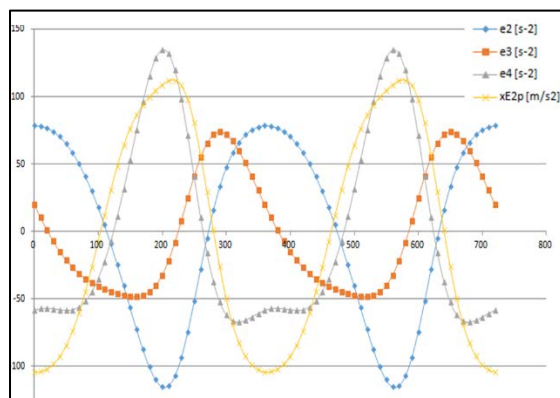


Figure 7: Variation of accelerations depending on the rotation angle FI1

The diagrams in Figure 8 show the forces in the couplings, which are generally called the reactions in the kinematic couples of the mechanism.

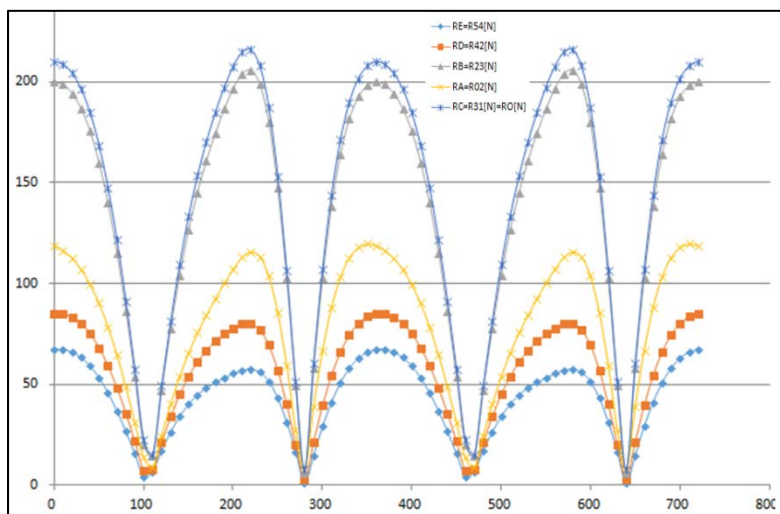


Figure 8: Forces in the couplings, which are generally called the reactions in the kinematic couples of the mechanism

To be able to solve the equations of motion of the machine, to obtain the (real) dynamic parameters of the motion when the angular input speed  $w_1 = wd$  is no longer considered constant (such as that given by the engine speed), but a value that varies depending on the dynamics of the mechanism together with the position occupied by the entry angle in the mechanism FI1, it is necessary to know the values of the mechanical moment of inertia  $J^*$  of the whole robot mechanism reduced to a single conducting element (element 1) and the value of its derivative in depending on the position angle FI1, ie  $J^{**}$  (Figure 9).

Likewise, the  $\epsilon_{s1}=\epsilon_{sd}$  input acceleration will be a variable and different from the zero value. Dynamic variations are produced by three causes: 1) variation of inertia forces in the mechanism; 2) the influence of kinematic couples; 3) the elastic deformations that occur in the elements of the moving mechanism. Because the largest share in the dynamics of a mechanism has the influence of variable inertia forces, in this paper we will consider only this parameter, theoretically determining a model that considers only the partial dynamics of the mechanism due to the influence of inertia forces within the robot mechanism.

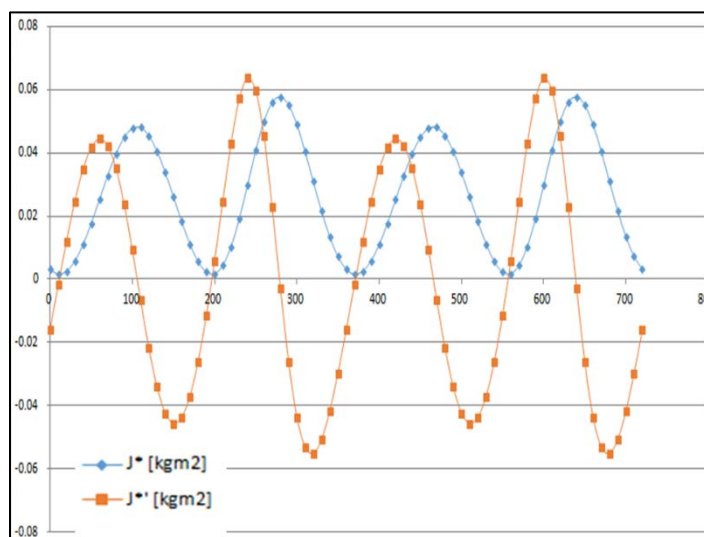


Figure 9: The moment of inertia (massic)  $J^*$  [ $\text{kg} \cdot \text{m}^2$ ] of the whole mechanism reduced to the crank 1, and the value of its derivative as a function of the position angle  $FI_1$ ,  $J^{*\prime}$  [ $\text{kg} \cdot \text{m}^2$ ].

Using the equations of motion of machine I and II (13), the original shapes generated by the authors of the paper, we can now draw the variation diagrams of the variable angular velocity of the crank  $wd$  [ $\text{s}^{-1}$ ] (Figure 10), and its acceleration  $epsd$  [ $\text{s}^{-2}$ ] (Figure 11), depending on the position angle of the crank 1,  $FI_1$ .

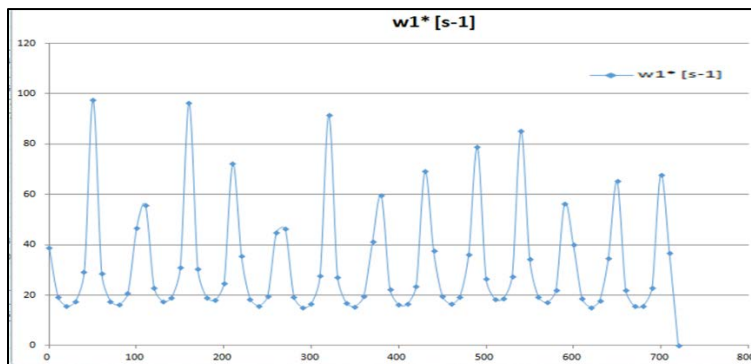


Figure 10: The variable angular velocity of the crank  $wd$  [ $\text{s}^{-1}$ ] for a nominal value of the engine speed  $nn = 200$  [rpm].

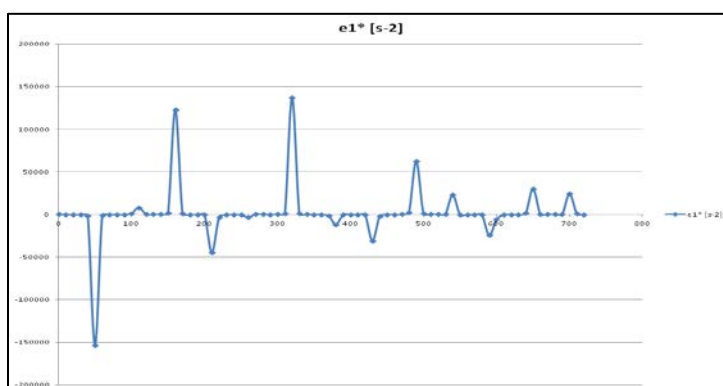


Figure 11: The variable angular acceleration of the crank  $ed$  [ $\text{s}^{-2}$ ] for a nominal value of the engine speed  $nn = 200$  [rpm].

Even if the diagram of theoretical dynamic angular accelerations looks like the measured ones (ie it looks like a vibration), its very high values are justified by the high nominal speed chosen at the robot input,  $n_1 = 200$  [rpm], these values decreasing considerably when the speed of element 1 (speed of crank 1) is decreased ten times, to only  $n_1 = 20$  [rot/min] (Figure 12).

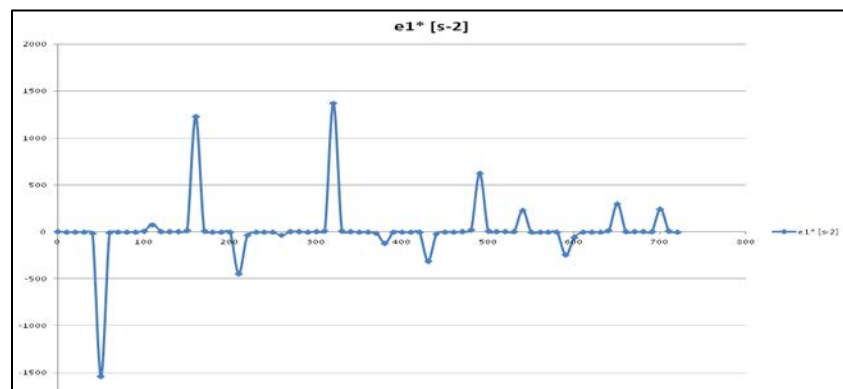


Figure 12: The variable angular acceleration of the crank  $e_1$   $[s^{-2}]$  for a nominal value of the engine speed  $n_n = 20$  [rpm].

The real velocities, given by the partial dynamic kinematics (14), can be visualized in the superimposed diagrams from figure 13.

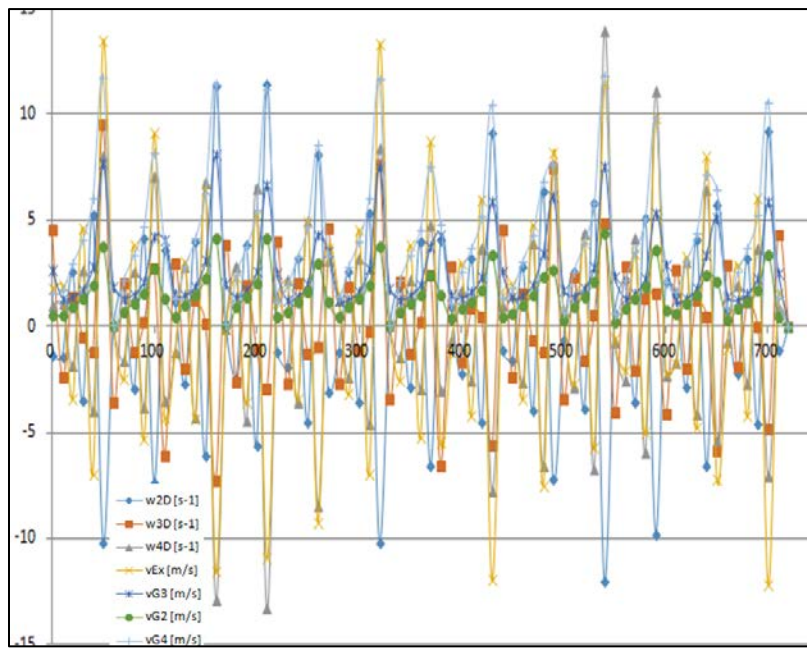


Figure 13: The dynamic velocities, given by the partial dynamic kinematics

Figures 14-17 show a comparative variation of kinematic and dynamic speeds.

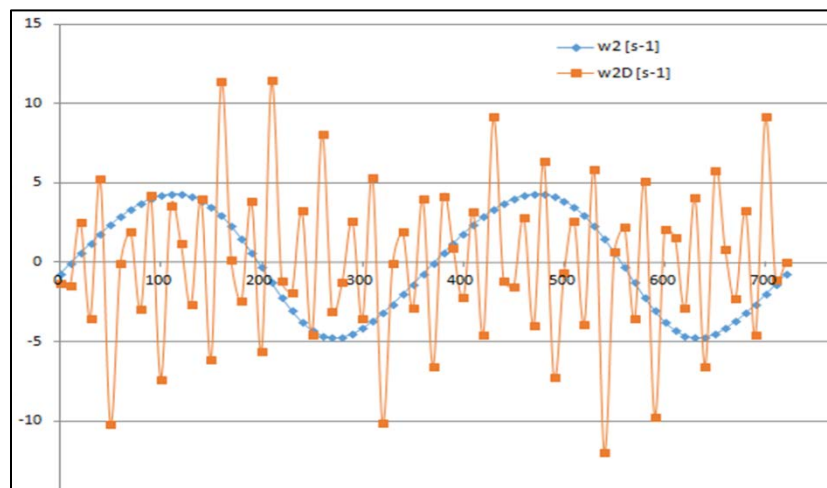


Figure 14: Comparative variation of kinematic and dynamic w2 speeds

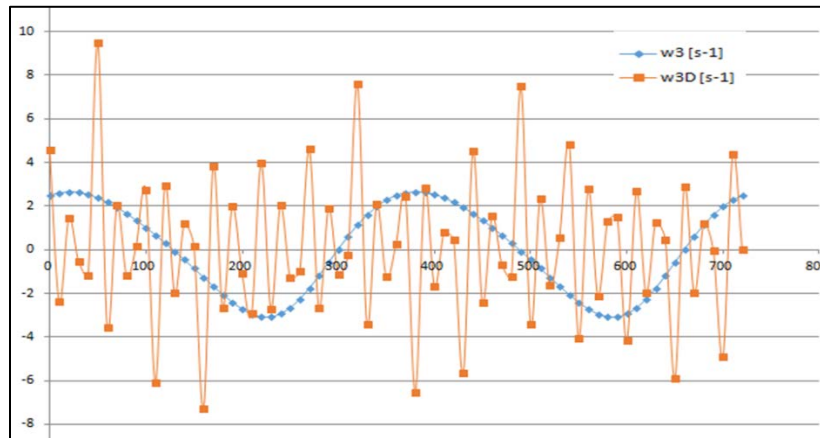


Figure 15: Comparative variation of kinematic and dynamic w3 speeds

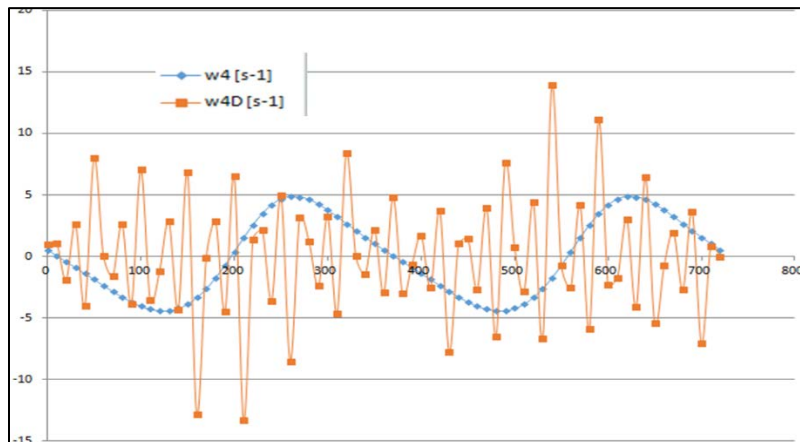


Figure 16: Comparative variation of kinematic and dynamic w4 speeds

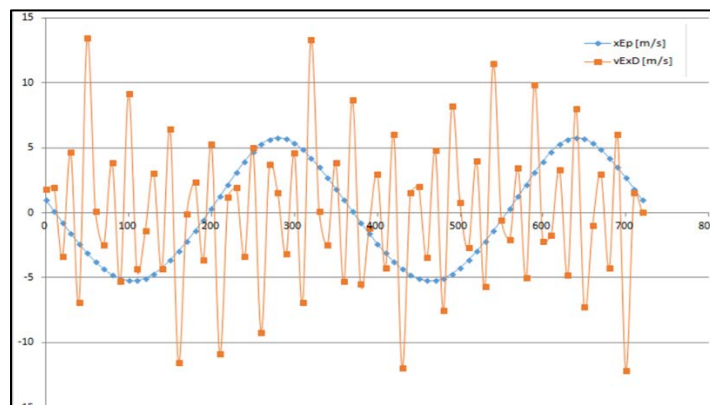


Figure 17: Comparative variation of kinematic and dynamic vE speeds

#### 4. CONCLUSIONS

Conveyor robots today have important roles in industry, being used to transport heavy objects within the sections of a plant, or between areas of the same section, from one work stand to another. Such structures can also be used to handle heavy objects, by lifting and rotating them from one work stand to another close, or from a supply belt to a stand.

The paper analyzes such a robot from a geometro-kinematic point of view, the forces acting on it in its kinematic couples, its dynamics influenced by the masses of the moving mechanism, practically by the inertial forces in the mechanism.

Such a classic 1T6R structure can be used simply, having a single degree of mobility, it acting within a plane, which is fixed on a movable central column that rotates the structure around the axis of the column.

Quite large variations occur between the kinematic parameters and the kinematic-dynamic ones, which increase with increasing speed of the crank 1 driven by the motor 1 which sets the whole system in motion. For low speeds the influence of dynamic parameters is relatively low.

The paper analyzes several dynamic aspects, such as the forces in the mechanism, the reactions in the couplings, due to inertia forces, mass inertial moments, reduced moment of inertia at crank 1, its derivative in relation to the rotation angle of the crank, equations of motion of machine I and II in an original form, which generates variable angular velocity, respectively variable angular acceleration, both made dynamically by crank 1, then determine the dynamic speeds and accelerations, taking into account the dynamic calculations of the influence of variation of inertia forces in the mechanism.

## 5. ACKNOWLEDGEMENT

This text was acknowledged and appreciated by Dr. Veturia CHIROIU Honorific member of Technical Sciences Academy of Romania (ASTR) PhD supervisor in Mechanical Engineering.

## 6. FUNDING INFORMATION

- a) 1-Research contract: Contract number 36-5-4D/1986 from 24IV1985, beneficiary CNST RO (Romanian National Center for Science and Technology) Improving dynamic mechanisms.
- b) 2-Contract research integration. 19-91-3 from 29.03.1991; Beneficiary: MIS; TOPIC: Research on designing mechanisms with bars, cams and gears, with application in industrial robots.
- c) 3-Contract research. GR 69/10.05.2007: NURC in 2762; theme 8: Dynamic analysis of mechanisms and manipulators with bars and gears.
- d) 4-Labor contract, no. 35/22.01.2013, the UPB, "Stand for reading performance parameters of kinematics and dynamic mechanisms, using inductive and incremental encoders, to a Mitsubishi Mechatronic System" "PN-II-IN-CI-2012-1-0389".
- e) All these matters are copyrighted! Copyrights: 394-qodGnhhtej, from 17-02-2010 13:42:18; 463-vpstuCGsiy, from 20-03-2010 12:45:30; 631-sqfsgqvutm, from 24-05-2010 16:15:22; 933-CrDztEfqow, from 07-01-2011 13:37:52.

## 7. ETHICS

Authors should address any ethical issues that may arise after the publication of this manuscript.

## REFERENCES

Antonescu, P., & Petrescu, F. I. T. (1985). An analytical method of synthesis of cam mechanism and flat stick. **Proceedings of the 4th International Symposium on Theory and Practice of Mechanisms**(TPM' 89), Bucharest.

Antonescu, P., & Petrescu, F. I. T. (1989). Contributions to kinetoplast dynamic analysis of distribution mechanisms. **SYROM'89**, Bucharest.

Antonescu, P., Oprean, M., & Petrescu, F. I. T. (1985a). Contributions to the synthesis of oscillating cam mechanism and oscillating flat stick. **Proceedings of the 4th International Symposium on Theory and Practice of Mechanisms**(TPM' 85), Bucharest.

Antonescu, P., Oprean, M., & Petrescu, F. I. T. (1985b). At the projection of the oscillate cams, there are mechanisms and distribution variables. **Proceedings of the 5th Conference of Engines, Automobiles, Tractors and Agricultural Machines**(TAM' 58), I-Motors and Cars, Brasov.

Antonescu, P., Oprean, M., & Petrescu, F. I. T. (1986). Projection of the profile of the rotating camshaft acting on the oscillating plate with disengagement. **Proceedings of the 3rd National Computer-aided Design Symposium in the field of Mechanisms and Machine Parts**(MMP' 86), Brasov.

Antonescu, P., Oprean, M., & Petrescu, F. I. T. (1987). Dynamic analysis of the cam distribution mechanisms. **Proceedings of the 7th National Symposium on Industrial Robots and Space Mechanisms**(RSM' 87), Bucharest.

Antonescu, P., Oprean, M., & Petrescu, F. I. T. (1988). **Analytical synthesis of Kurz profile**, rotating the flat cam. Mach, Build. Rev.

Antonescu, P., Petrescu, F. I. T., & Antonescu, O. (1994). **Contributions to the synthesis of the rotating cam mechanism and the tip of the balancing tip**. Brasov.

Antonescu, P., Petrescu, F. I. T., & Antonescu, O. (1997) Geometrical synthesis of the rotary cam and balance tappet mechanism. **Bucharest**, (3), 23-23.

Antonescu, P., Petrescu, F. I. T., & Antonescu, O. (2000a). Contributions to the synthesis of the rotary disc-cam profile. **Proceedings of the 8th International Conference on the Theory of Machines and Mechanisms**(TMM' 00), Liberec, Czech Republic), 51-56.

Antonescu, P., Petrescu, F. I. T., & Antonescu, O. (2000b). Synthesis of the rotary cam profile with balance follower. **Proceedings of the 8th Symposium on Mechanisms and Mechanical Transmissions**(MMT' 00), Timișoara, 39-44.

Antonescu, P., Petrescu, F. I. T., & Antonescu, O. (2001). Contributions to the synthesis of mechanisms with rotary disc-cam. **Proceedings of the 8th IFToMM International Symposium on Theory of Machines and Mechanisms**(TMM' 01), Bucharest, ROMANIA, 31-36.

Atefi, G., Abdous, M. A., & Ganjehkaviri, A. (2008). Analytical Solution of Temperature Field in Hollow Cylinder under Time Dependent Boundary Condition Using Fourier series, **Am. J. Eng. Applied Sci.**, 1(2), 141-148. DOI: 10.3844/ajeassp.2008.141.148

Avaei, A., Ghotbi, A. R., & Aryafar, M. (2008). Investigation of Pile-Soil Interaction Subjected to Lateral Loads in Layered Soils, **Am. J. Eng. Applied Sci.**, 1(1), 76-81. DOI: 10.3844/ajeassp.2008.76.81

Aversa, R., Petrescu, R. V. V., Apicella, A., & Petrescu, F. I. T. (2017a). Nano-diamond hybrid materials for structural biomedical application. **Am. J. Biochem. Biotechnol.**, (13), 34-41. DOI: 10.3844/ajbbsp.2017.34.41

Aversa, R., Petrescu, R. V. V., Akash, B., Bucinell, R. B., & Corchado, J. M. (2017b). Kinematics and forces to a new model forging manipulator. **Am. J. Applied Sci.**, (14), 60-80. DOI: 10.3844/ajassp.2017.60.80

Aversa, R., Petrescu, R. V. V., Apicella, A., Petrescu, F. I. T. & Calautit, J. K. (2017c). Something about the V engines design. **Am. J. Applied Sci.**, (14), 34-52. DOI: 10.3844/ajassp.2017.34.52



Aversa, R., Parcesepe, D., Petrescu, R. V. V., Berto, F., & Chen, G. (2017d). Process ability of bulk metallic glasses. **Am. J. Applied Sci.**, (14), 294-301. DOI: 10.3844/ajassp.2017.294.301

Aversa, R., Petrescu, R. V. V., Akash, B., Bucinell, R. B., & Corchado, J. M. (2017e). Something about the balancing of thermal motors. **Am. J. Eng. Applied Sci.**, (10), 200-217. DOI: 10.3844/ajeassp.2017.200.217

Aversa, R., Petrescu, F. I. T., Petrescu, R. V. V., & Apicella, A. (2016a). Biomimetic FEA bone modeling for customized hybrid biological prostheses development. **Am. J. Applied Sci.**, (13), 1060-1067. DOI: 10.3844/ajassp.2016.1060.1067

Aversa, R., Parcesepe, D., Petrescu, R. V. V., G. Chen, G. & Petrescu, F. I. T. (2016b). Glassy amorphous metal injection molded induced morphological defects. **Am. J. Applied Sci.**, (13), 1476-1482. DOI: 10.3844/ajassp.2016.1476.1482

Aversa, R., Petrescu, R. V. V., Petrescu, F. I. T., & Apicella, A., (2016c). Smart-factory: Optimization and process control of composite centrifuged pipes. **Am. J. Applied Sci.**, (13), 1330-1341. DOI: 10.3844/ajassp.2016.1330.1341

Aversa, R., Tamburrino, F., Petrescu, R. V. V., Petrescu, F. I. T., & Artur, M. (2016d). Biomechanically inspired shape memory effect machines driven by muscle like acting NiTi alloys. **Am. J. Applied Sci.**, (13), 1264-1271. DOI: 10.3844/ajassp.2016.1264.1271

Aversa, R., Buzea, E. M., Petrescu, R. V. V., Apicella, A., & Neacsă, M. (2016e). Present a mechatronic system having able to determine the concentration of carotenoids. **Am. J. Eng. Applied Sci.**, (9), 1106-1111. DOI: 10.3844/ajeassp.2016.1106.1111

Aversa, R., Petrescu, R. V. V., Sorrentino, R., Petrescu, F. I. T., & Apicella, A. (2016f). Hybrid ceramo-polymeric nanocomposite for biomimetic scaffolds design and preparation. **Am. J. Eng. Applied Sci.**, (9), 1096-1105. DOI: 10.3844/ajeassp.2016.1096.1105

Aversa, R., Perrotta, V., Petrescu, R. V. V., Misiano, C., & Petrescu, F. I. T. (2016g). From structural colors to super-hydrophobicity and achromatic transparent protective coatings: Ion plating plasma assisted TiO<sub>2</sub> and SiO<sub>2</sub> nano-film deposition. **Am. J. Eng. Applied Sci.**, (9), 1037-1045. DOI: 10.3844/ajeassp.2016.1037.1045

Aversa, R., Petrescu, R. V. V., Petrescu, F. I. T., & Apicella, A. (2016h). Biomimetic and evolutionary design driven innovation in sustainable products development. **Am. J. Eng. Applied Sci.**, (9), 1027-1036. DOI: 10.3844/ajeassp.2016.1027.1036

Aversa, R., Petrescu, R. V. V., Apicella, A., & Petrescu, F. I. T. (2016i). Mitochondria are naturally micro robots - a review. **Am. J. Eng. Applied Sci.**, (9), 991-1002. DOI: 10.3844/ajeassp.2016.991.1002

Aversa, R., Petrescu, R. V. V., Apicella, A., & Petrescu, F. I. T. (2016j). We are addicted to vitamins C and E-A review. **Am. J. Eng. Applied Sci.**, (9), 1003-1018. DOI: 10.3844/ajeassp.2016.1003.1018

Aversa, R., Petrescu, R. V. V., Apicella, A., & Petrescu, F. I. T. (2016k). Physiologic human fluids and swelling behavior of hydrophilic biocompatible hybrid ceramo-polymeric materials. **Am. J. Eng. Applied Sci.**, (9), 962-972. DOI: 10.3844/ajeassp.2016.962.972

Aversa, R., Petrescu, R. V. V., Apicella, A., & Petrescu, F. I. T. (2016l). One can slow down the aging through antioxidants. **Am. J. Eng. Applied Sci.**, (9), 1112-1126. DOI: 10.3844/ajeassp.2016.1112.1126



Aversa, R., Petrescu, R. V. V., Apicella, A., & Petrescu, F. I. T. (2016m). About homeopathy or «*Similia Similibus Curentur*». **Am. J. Eng. Applied Sci.**, (9), 1164-1172. DOI: 10.3844/ajeassp.2016.1164.1172

Aversa, R., Petrescu, R. V. V., Apicella, A., & Petrescu, F. I. T. (2016n). The basic elements of life's. **Am. J. Eng. Applied Sci.**, (9), 1189-1197. DOI: 10.3844/ajeassp.2016.1189.1197

Aversa, R., Petrescu, F. I. T., Petrescu, R. V. V., & Apicella, A. (2016o). Flexible stem trabecular prostheses. **Am. J. Eng. Applied Sci.**, (9), 1213-1221. DOI: 10.3844/ajeassp.2016.1213.122

Azaga, M., & Othman, M. (2008). Source Couple Logic (SCL): Theory and Physical Design, **Am. J. Eng. Applied Sci.**, 1(1), 24-32. DOI: 10.3844/ajeassp.2008.24.32

Cao, W., Ding, H., Bin, Z., & Ziming, C. (2013). New structural representation and digital-analysis platform for symmetrical parallel mechanisms. **Int. J. Adv. Robotic Sys.** DOI: 10.5772/56380

Comanescu, A. (2010). Bazele Modelarii Mecanismelor. 1st Edn., **E. Politeh, Press**, Bucureşti, pp: 274.

Dong, H., Giakoumidis, N., Figueroa, N., & Mavridis, N. (2013). Approaching behaviour monitor and vibration indication in developing a General Moving Object Alarm System (GMOAS). **Int. J. Adv. Robotic Sys.** DOI: 10.5772/56586

Yousif El-Tous (2008). Pitch Angle Control of Variable Speed Wind Turbine, **Am. J. Eng. Applied Sci.**, 1(2), 118-120. DOI: 10.3844/ajeassp.2008.118.120

Franklin, D. J. (1930). Ingenious Mechanisms for Designers and Inventors. 1st Edn., **Industrial Press Publisher**.

He, B., Wang, Z., Li, Q., Xie, H., & Shen, R. (2013). An analytic method for the kinematics and dynamics of a multiple-backbone continuum robot. **IJARS**. DOI: 10.5772/54051

Jolgaf, M., Sulaiman, S. B., M.K.A Ariffin, M. K. A., & Faieza, A. A. (2008). Closed Die Forging Geometrical Parameters Optimization for Al-MMC, **Am. J. Eng. Applied Sci.**, 1(1), 1-6. DOI : 10.3844/ajeassp.2008.1.6

Kannappan, A. N., Kesavasamy, R., & Ponnuswamy, V. (2008). Molecular Interaction Studies of H-Bonded Complexes of Benzamide in 1,4-Dioxan with Alcohols From Acoustic and Thermodynamic Parameters, **Am. J. Eng. Applied Sci.**, 1(2), 95-99. DOI: 10.3844/ajeassp.2008.95.99

Lee, B. J. (2013). Geometrical derivation of differential kinematics to calibrate model parameters of flexible manipulator. **Int. J. Adv. Robotic Sys.** DOI: 10.5772/55592

Lin, W., Li, B., Yang, X., & Zhang, D. (2013). Modelling and control of inverse dynamics for a 5-DOF parallel kinematic polishing machine. **Int. J. Adv. Robotic Sys.** DOI: 10.5772/54966

Liu, H., Zhou, W., Lai, X., & Zhu, S. (2013). An efficient inverse kinematic algorithm for a PUMA560-structured robot manipulator. **IJARS**. DOI: 10.5772/56403

Meena, P., & Rittidech, S. (2008). Comparisons of Heat Transfer Performance of a Closed-looped Oscillating Heat Pipe and Closed-looped Oscillating Heat Pipe with Check Valves Heat Exchangers, **Am. J. Eng. Applied Sci.**, 1(1), 7-11. DOI: 10.3844/ajeassp.2008.7.11



Meena, P., Rittidech, S., & Tammasaeng, P. (2008). Effect of Inner Diameter and Inclination Angles on Operation Limit of Closed-Loop Oscillating Heat-Pipes with Check Valves, **Am. J. Eng. Applied Sci.**, 1(2), 100-103. DOI: 10.3844/ajeassp.2008.100.103

Mirsayar, M. M., Joneidi, A., Petrescu, R. V. V., Petrescu, F. I. T., & Berto, F. (2017). Extended MTSN criterion for fracture analysis of soda lime glass. **Eng. Fracture Mechan.**(178), 50-59. DOI: 10.1016/j.engfracmech.2017.04.018

Ng, K. C., Yusoff,M. Z., Munisamy, K., Hasini, H., & Shuaib, N. H. (2008). Time-Marching Method for Computations of High-Speed Compressible Flow on Structured and Unstructured Grid, **Am. J. Eng. Applied Sci.**, 1(2), 89-94. DOI: 10.3844/ajeassp.2008.89.94

Padula, F., & Perdereau, V. (2013). An on-line path planner for industrial manipulators. **Int. J. Adv. Robotic Sys.** DOI: 10.5772/55063

Pannirselvam, N., Raghunath, P. N., & Suguna, K. (2008). Neural Network for Performance of Glass Fibre Reinforced Polymer Plated RC Beams, **Am. J. Eng. Applied Sci.**, 1(1), 82-88. DOI: 10.3844/ajeassp.2008.82.88

Perumaal, S., & Jawahar, N. (2013). Automated trajectory planner of industrial robot for pick-and-place task. **IJARS**. DOI: 10.5772/53940

Petrescu, F. I. T., & Petrescu, R. V. V. (1995a). **Contributions to optimization of the polynomial motion laws of the stick from the internal combustion engine distribution mechanism**. Bucharest, (1), 249-256.

Petrescu, F. I. T., & Petrescu, R. V. V. (1995b). **Contributions to the synthesis of internal combustion engine distribution mechanisms**. Bucharest, (1), 257-264.

Petrescu, F. I. T., & Petrescu, R. V. V. (1997a). **Dynamics of cam mechanisms (exemplified on the classic distribution mechanism)**. Bucharest, (3), 353-358.

Petrescu, F. I. T., & Petrescu, R. V. V. (1997b). **Contributions to the synthesis of the distribution mechanisms of internal combustion engines with a Cartesian coordinate method**. Bucharest, (3), 359-364.

Petrescu, F. I. T., & Petrescu, R. V. V. (1997c). **Contributions to maximizing polynomial laws for the active stroke of the distribution mechanism from internal combustion engines**. Bucharest, (3), 365-370.

Petrescu, F. I. T., & Petrescu, R. V. V. (2000a). Synthesis of distribution mechanisms by the rectangular (Cartesian) coordinate method. **Proceedings of the 8th National Conference on International Participation(CIP' 00)**, Craiova, Romania, 297-302.

Petrescu, F. I. T., & Petrescu, R. V. V. (2000b). The design (synthesis) of cams using the polar coordinate method (triangle method). **Proceedings of the 8th National Conference on International Participation(CIP' 00)**, Craiova, Romania, 291-296.

Petrescu, F. I. T., & Petrescu, R. V. V. (2002a). Motion laws for cams. Proceedings of the International Computer Assisted Design, **National Symposium Participation(SNP' 02)**, Brașov, 321-326.

Petrescu, F. I. T., & Petrescu, R. V. V. (2002b). Camshaft dynamics elements. **Proceedings of the International Computer Assisted Design, National Participation Symposium(SNP' 02)**, Brașov, 327-332.



Petrescu, F. I. T., & Petrescu, R. V. V. (2003). Some elements regarding the improvement of the engine design. **Proceedings of the National Symposium, Descriptive Geometry, Technical Graphics and Design(GTD' 03)**, Brașov, 353-358.

Petrescu, F. I. T., & Petrescu, R. V. V. (2005a). The cam design for a better efficiency. **Proceedings of the International Conference on Engineering Graphics and Design(EGD' 05)**, Bucharest, 245-248.

Petrescu, F. I. T., & Petrescu, R. V. V. (2005b). Contributions at the dynamics of cams. **Proceedings of the 9th IFToMM International Symposium on Theory of Machines and Mechanisms(TMM' 05)**, Bucharest, Romania, 123-128.

Petrescu, F. I. T., & Petrescu, R. V. V. (2005c). Determining the dynamic efficiency of cams. **Proceedings of the 9th IFToMM International Symposium on Theory of Machines and Mechanisms(TMM' 05)**, Bucharest, Romania, 129-134.

Petrescu, F. I. T., & Petrescu, R. V. V. (2005d). An original internal combustion engine. **Proceedings of the 9th IFToMM International Symposium on Theory of Machines and Mechanisms(TMM' 05)**, Bucharest, Romania, 135-140.

Petrescu, F. I. T., & Petrescu, R. V. V. (2005e). Determining the mechanical efficiency of Otto engine's mechanism. **Proceedings of the 9th IFToMM International Symposium on Theory of Machines and Mechanisms(TMM 05)**, Bucharest, Romania, 141-146.

Petrescu, F. I. T., & Petrescu, R. V. V. (2011a). Mechanical Systems, Serial and Parallel (Romanian). 1st Edn., **LULU Publisher**, London, UK), 124.

Petrescu, F. I. T., & Petrescu, R. V. V. (2011b). Trenuri Planetare. **Createspace Independent Pub.**, 104 pages, ISBN-13: 978-1468030419.

Petrescu, F. I. T., & Petrescu, R. V. V. (2012a). Kinematics of the planar quadrilateral mechanism. **ENGEVISTA(14)**, 345-348.

Petrescu, F. I. T., & Petrescu, R. V. V. (2012b). Mecatronica-Sisteme Seriale si Paralele. 1st Edn., **Create Space Publisher**, USA), 128.

Petrescu, F. I. T., Petrescu, R. V. V. (2013a). Cinematics of the 3R dyad. **ENGEVISTA(15)**, 118-124.

Petrescu, F. I. T., & Petrescu, R. V. V. (2013b). Forces and efficiency of cams. **Int. Rev. Mechanical Eng.**

Petrescu, F. I. T., & Petrescu, R. V. V. (2016a). Parallel moving mechanical systems kinematics. **ENGEVISTA**, (18), 455-491.

Petrescu, F. I. T., & Petrescu, R. V. V. (2016b). Direct and inverse kinematics to the anthropomorphic robots. **ENGEVISTA**, (18), 109-124.

Petrescu, F. I. T., & Petrescu, R. V. V. (2016c). Dynamic cinematic to a structure 2R. **Revista Geintec-Gestao Inovacao E Tecnol.**, (6), 3143-3154.

Petrescu, F. I. T., Grecu, B., Comanescu, A., & Petrescu, R. V. V. (2009). Some mechanical design elements. **Proceeding of the International Conference on Computational Mechanics and Virtual Engineering(MVE' 09)**, Brașov, 520-525.

Petrescu, F. I. T. (2011). Teoria Mecanismelor si a Masinilor: Curs Si Aplicatii. 1st Edn., **CreateSpace Independent Publishing Platform**. ISBN-10: 1468015826. P. 432.



- Petrescu, F. I. T. (2015a). Geometrical synthesis of the distribution mechanisms. **Am. J. Eng. Applied Sci.**, (8), 63-81. DOI: 10.3844/ajeassp.2015.63.81
- Petrescu, F. I. T. (2015b). Machine motion equations at the internal combustion heat engines. **Am. J. Eng. Applied Sci.**, 8: 127-137. DOI: 10.3844/ajeassp.2015.127.137
- Petrescu, R. V. V., Aversa, R., Apicella, A., & Petrescu, F. I. T. (2016). Future medicine services robotics. **Am. J. Eng. Applied Sci.**, (9), 1062-1087. DOI: 10.3844/ajeassp.2016.1062.1087
- Petrescu, R. V. V., Aversa, R., Akash, B., Bucinell, R., & Corchado, J. (2017a). Yield at thermal engines internal combustion. **Am. J. Eng. Applied Sci.**, (10), 243-251. DOI: 10.3844/ajeassp.2017.243.251
- Petrescu, R. V. V., Aversa, R., Akash, B., Ronald, B., & Corchado, J. (2017b). Velocities and accelerations at the 3R mechatronic systems. **Am. J. Eng. Applied Sci.**, (10), 252-263. DOI: 10.3844/ajeassp.2017.252.263
- Petrescu, R. V. V., Aversa, R., Akash, B., Bucinell, R., & Corchado, J. (2017c). Anthropomorphic solid structures n-r kinematics. **Am. J. Eng. Applied Sci.**(10), 279-291. DOI: 10.3844/ajeassp.2017.279.291
- Petrescu, R. V. V., Aversa, R., Akash, B., Bucinell, R., & Corchado, J. (2017d). Inverse kinematics at the anthropomorphic robots, by a trigonometric method. **Am. J. Eng. Applied Sci.**(10), 394-411. DOI: 10.3844/ajeassp.2017.394.411
- Petrescu, R. V. V., Aversa, R., Akash, B., Bucinell, R., & Corchado, J. (2017e). Forces at internal combustion engines. **Am. J. Eng. Applied Sci.**(10), 382-393. DOI: 10.3844/ajeassp.2017.382.393
- Petrescu, R. V. V., Aversa, R., Akash, B., Bucinell, R., & Corchado, J. (2017f). Gears-Part I. **Am. J. Eng. Applied Sci.**(10), 457-472. DOI: 10.3844/ajeassp.2017.457.472
- Petrescu, R. V. V., Aversa, R., Akash, B., Bucinell, R., & Corchado, J. (2017g). Gears-part II. **Am. J. Eng. Applied Sci.**(10), 473-483. DOI: 10.3844/ajeassp.2017.473.483
- Petrescu, R. V. V., Aversa, R., Akash, B., Bucinell, R., & Corchado, J. (2017h). Cam-gears forces, velocities, powers and efficiency. **Am. J. Eng. Applied Sci.**(10), 491-505. DOI: 10.3844/ajeassp.2017.491.505
- Petrescu, R. V. V., Aversa, R., Akash, B., Bucinell, R., & Corchado, J. (2017i). Dynamics of mechanisms with cams illustrated in the classical distribution. **Am. J. Eng. Applied Sci.**(10), 551-567. DOI: 10.3844/ajeassp.2017.551.567
- Petrescu, R. V. V., Aversa, R., Akash, B., Bucinell, R., & Corchado, J. (2017j). Testing by non-destructive control. **Am. J. Eng. Applied Sci.**, (10), 568-583. DOI: 10.3844/ajeassp.2017.568.583
- Petrescu, R. V. V., Aversa, R., Apicella, A., & Petrescu, F. I. T. (2017k). Transportation engineering. **Am. J. Eng. Applied Sci.**, (10), 685-702. DOI: 10.3844/ajeassp.2017.685.702
- Petrescu, R. V. V., Aversa, R., Kozaitis, S., Apicella, A., & Petrescu, F. I. T. (2017l). The quality of transport and environmental protection, part I. **Am. J. Eng. Applied Sci.**, (10), 738-755. DOI: 10.3844/ajeassp.2017.738.755



Petrescu, R. V. V., Aversa, R., Akash, B., R. Bucinell, R., & Corchado, J. (2017m). Modern propulsions for aerospace-a review. **J. Aircraft Spacecraft Technol.**, (1), 1-8. DOI: 10.3844/jastsp.2017.1.8

Petrescu, R. V. V., Aversa, R., Akash, B., Bucinell, R., & Corchado, J. (2017n). Modern propulsions for aerospace-part II. **J. Aircraft Spacecraft Technol.**, (1), 9-17. DOI: 10.3844/jastsp.2017.9.17

Petrescu, R. V. V., Aversa, R., Akash, B., Bucinell, R., & Corchado, J. (2017o). History of aviation-a short review. **J. Aircraft Spacecraft Technol.**, (1), 30-49. DOI: 10.3844/jastsp.2017.30.49

Petrescu, R. V. V., Aversa, R., Akash, B., Bucinell, R., & Corchado, J. (2017p). Lockheed martin-a short review. **J. Aircraft Spacecraft Technol.**, (1), 50-68. DOI: 10.3844/jastsp.2017.50.68

Petrescu, R. V. V., Aversa, R., Akash, B., Bucinell, R., & Corchado, J. (2017q). Our universe. **J. Aircraft Spacecraft Technol.**, (1), 69-79. DOI: 10.3844/jastsp.2017.69.79

Petrescu, R. V. V., Aversa, R., Akash, B., Corchado, J., & Berto, F. (2017r). What is a UFO? **J. Aircraft Spacecraft Technol.**, (1), 80-90. DOI: 10.3844/jastsp.2017.80.90

Petrescu, R. V. V., Aversa, R., Akash, B., Corchado, J., & Berto, F. (2017s). About bell helicopter FCX-001 concept aircraft-a short review. **J. Aircraft Spacecraft Technol.**, (1), 91-96. DOI: 10.3844/jastsp.2017.91.96

Petrescu, R. V. V., Aversa, R., Akash, B., Corchado, J., & Berto, F. (2017t). Home at airbus. **J. Aircraft Spacecraft Technol.**, (1), 97-118. DOI: 10.3844/jastsp.2017.97.118

Petrescu, R. V. V., Aversa, R., Akash, B., Corchado, J., & Berto, F. (2017u). Airlander. **J. Aircraft Spacecraft Technol.**, (1), 119-148. DOI: 10.3844/jastsp.2017.119.148

Petrescu, R. V. V., Ersa, R., Akash, B., Corchado, J., & Berto, F. (2017v). When boeing is dreaming-a review. **J. Aircraft Spacecraft Technol.**, (1), 149-161. DOI: 10.3844/jastsp.2017.149.161

Petrescu, R. V. V., Aversa, R., Akash, B., Corchado, J., & Berto, F. (2017w). About Northrop Grumman. **J. Aircraft Spacecraft Technol.**, (1), 162-185. DOI: 10.3844/jastsp.2017.162.185

Petrescu, R. V. V., Aversa, R., Akash, B., Corchado, J., & Berto, F. (2017x). Some special aircraft. **J. Aircraft Spacecraft Technol.**, (1), 186-203. DOI: 10.3844/jastsp.2017.186.203

Petrescu, R. V. V., Aversa, R., Akash, B., Corchado, J., & Berto, F. (2017y). About helicopters. **J. Aircraft Spacecraft Technol.**, (1), 204-223. DOI: 10.3844/jastsp.2017.204.223

Petrescu, R. V. V., Aversa, R., Akash, B., Berto, F., & Apicella, A. (2017z). The modern flight. **J. Aircraft Spacecraft Technol.**, (1), 224-233. DOI: 10.3844/jastsp.2017.224.233

Petrescu, R. V. V., Aversa, R., Akash, B., Berto, F., & Apicella, A. (2017aa). Sustainable energy for aerospace vessels. **J. Aircraft Spacecraft Technol.**, (1), 234-240. DOI: 10.3844/jastsp.2017.234.240

Petrescu, R. V. V., Aversa, R., Akash, B., Berto, F., & Apicella, A. (2017ab). Unmanned helicopters. **J. Aircraft Spacecraft Technol.**, (1), 241-248. DOI: 10.3844/jastsp.2017.241.248

Petrescu, R. V. V., Aversa, R., Akash, B., Berto, F., & Apicella, A. (2017ac). Project HARP. **J. Aircraft Spacecraft Technol.**, (1), 249-257. DOI: 10.3844/jastsp.2017.249.257



Petrescu, R. V. V., Aversa, R., Akash, B., Berto, F., & Apicella, A. (2017ad). Presentation of Romanian engineers who contributed to the development of global aeronautics-part I. **J. Aircraft Spacecraft Technol.**, (1), 258-271. DOI: 10.3844/jastsp.2017.258.271

Petrescu, R. V. V., Aversa, R., Akash, B., Berto, F., & Apicella, A. (2017ae). A first-class ticket to the planet mars, please. **J. Aircraft Spacecraft Technol.**, (1), 272-281. DOI: 10.3844/jastsp.2017.272.281

Petrescu, R. V. V., Aversa, R., Apicella, A., Mirsayar, M. M., & Kozaitis, S. (2018a). NASA started a propeller set on board voyager 1 after 37 years of break. **Am. J. Eng. Applied Sci.**, (11), 66-77. DOI: 10.3844/ajeassp.2018.66.77

Petrescu, R. V. V., Aversa, R., Apicella, A., Mirsayar, M. M., & Kozaitis, S. (2018b). There is life on mars? **Am. J. Eng. Applied Sci.**, (11), 78-91. DOI: 10.3844/ajeassp.2018.78.91

Petrescu, R. V. V., Aversa, R., Apicella, A., & Petrescu, F. I. T. (2018c). Friendly environmental transport. **Am. J. Eng. Applied Sci.**, (11), 154-165. DOI: 10.3844/ajeassp.2018.154.165

Petrescu, R. V. V., Aversa, R., Akash, B., Abu-Lebdeh, T. M., T. M., & Apicella, A. (2018d). Buses running on gas. **Am. J. Eng. Applied Sci.**, (11), 186-201. DOI: 10.3844/ajeassp.2018.186.201

Petrescu, R. V. V., Aversa, R., Akash, B., Abu-Lebdeh, T. M., T. M., & Apicella, A. (2018e). Some aspects of the structure of planar mechanisms. **Am. J. Eng. Applied Sci.**, (11), 245-259. DOI: 10.3844/ajeassp.2018.245.259

Petrescu, R. V. V., Aversa, R., Abu-Lebdeh, T. M., Apicella, A., & Petrescu, F. I. T. (2018f). The forces of a simple carrier manipulator. **Am. J. Eng. Applied Sci.**, (11), 260-272. DOI: 10.3844/ajeassp.2018.260.272

Petrescu, R. V. V., Aversa, R., Abu-Lebdeh, T. M., Apicella, A., & Petrescu, F. I. T. (2018g). The dynamics of the otto engine. **Am. J. Eng. Applied Sci.**, (11), 273-287. DOI: 10.3844/ajeassp.2018.273.287

Petrescu, R. V. V., Aversa, R., Abu-Lebdeh, T. M., Apicella, A., & Petrescu, F. I. T. (2018h). NASA satellites help us to quickly detect forest fires. **Am. J. Eng. Applied Sci.**, (11), 288-296. DOI: 10.3844/ajeassp.2018.288.296

Petrescu, R. V. V., Aversa, R., Abu-Lebdeh, T. M., Apicella, A., & Petrescu, F. I. T. (2018i). Kinematics of a mechanism with a triad. **Am. J. Eng. Applied Sci.**, (11), 297-308. DOI: 10.3844/ajeassp.2018.297.308

Petrescu, R. V. V., Aversa, R., Apicella, A., & Petrescu, F. I. T. (2018j). Romanian engineering "on the wings of the wind". **J. Aircraft Spacecraft Technol.**, (2), 1-18. DOI: 10.3844/jastsp.2018.1.18

Petrescu, R. V. V., Aversa, R., Apicella, A., & Petrescu, F. I. T. (2018k). NASA Data used to discover eighth planet circling distant star. **J. Aircraft Spacecraft Technol.**, (2), 19-30. DOI: 10.3844/jastsp.2018.19.30

Petrescu, R. V. V., Aversa, R., Apicella, A., & Petrescu, F. I. T. (2018l). NASA has found the most distant black hole. **J. Aircraft Spacecraft Technol.**, (2), 31-39. DOI: 10.3844/jastsp.2018.31.39



Petrescu, R. V. V., Aversa, R., Apicella, A., & Petrescu, F. I. T. (2018m). NASA selects concepts for a new mission to titan, the moon of saturn. **J. Aircraft Spacecraft Technol.**, (2), 40-52. DOI: 10.3844/jastsp.2018.40.52

Petrescu, R. V. V., Aversa, R., Apicella, A., & Petrescu, F. I. T. (2018n). NASA sees first in 2018 the direct proof of ozone hole recovery. **J. Aircraft Spacecraft Technol.**, (2), 53-64. DOI: 10.3844/jastsp.2018.53.64

Pourmahmoud, N. (2008). Rarefied Gas Flow Modeling inside Rotating Circular Cylinder, **Am. J. Eng. Applied Sci.**, 1(1), 62-65. DOI: 10.3844/ajeassp.2008.62.65

Rajasekaran, A., Raghunath, P. N., & Suguna, K. (2008). Effect of Confinement on the Axial Performance of Fibre Reinforced Polymer Wrapped RC Column, **Am. J. Eng. Applied Sci.**, 1(2), 110-117. DOI: 10.3844/ajeassp.2008.110.117

Shojaeeefard, M. H., Goudarzi, K., Noorpoor, A. R., & Fazelpour, M. (2008). A Study of Thermal Contact using Nonlinear System Identification Models, **Am. J. Eng. Applied Sci.**, 1(1), 16-23. DOI: 10.3844/ajeassp.2008.16.23

Taher, S. A., Hematti, R., & Nemati, M. (2008). Comparison of Different Control Strategies in GA-Based Optimized UPFC Controller in Electric Power Systems, **Am. J. Eng. Applied Sci.**, 1(1), 45-52. DOI: 10.3844/ajeassp.2008.45.52

Tavallaei, M. A., & Tousi, B. (2008). Closed Form Solution to an Optimal Control Problem by Orthogonal Polynomial Expansion, **Am. J. Eng. Applied Sci.**, 1(2), 104-109. DOI: 10.3844/ajeassp.2008.104.109

Theansuwan, W., & Triratanasirichai, K. (2008). Air Blast Freezing of Lime Juice: Effect of Processing Parameters, **Am. J. Eng. Applied Sci.**, 1(1), 33-39. DOI: 10.3844/ajeassp.2008.33.39

Zahedi, S. A., Vaezi, M., & Tolou, N. (2008). Nonlinear Whitham-Broer-Kaup Wave Equation in an Analytical Solution, **Am. J. Eng. Applied Sci.**, 1(2), 161-167. DOI: 10.3844/ajeassp.2008.161.167

Zulkifli, R., Sopian, K., Abdullah, S., & Takriff, M. S. (2008). Effect of Pulsating Circular Hot Air Jet Frequencies on Local and Average Nusselt Number, **Am. J. Eng. Applied Sci.**, 1(1), 57-61. DOI: 10.3844/ajeassp.2008.57.61

